
[View Journal Online](#)  
[View Article Online](#)

# Orange to red emissive aldehyde substituted donor- $\pi$ -acceptor phenothiazine derivatives: Optoelectronic, DFT and thermal studies

Shivaraj Mantur <sup>1</sup>, Mallikarjun Kalagouda Patil <sup>2</sup>, Afra Quasar Abdul Rasheed Nadaf <sup>1,3</sup>, Mahesh Sadashivappa Najare <sup>1</sup>, Mohammed Yaseen <sup>1</sup>, Aravind Raviraj Nesaragi <sup>1</sup>, Sanjeev Ramchandra Inamdar <sup>2</sup>, Imtiyaz Ahmed Khazi <sup>1</sup> and Ravindra Ramappa Kamble <sup>1,\*</sup>

<sup>1</sup> Department of Chemistry, Karnatak University, Dharwad 580003, Karnataka, India

<sup>2</sup> Laser Spectroscopy Program, Department of Physics, Karnatak University, Dharwad, 580003, India

<sup>3</sup> Department of Chemistry, Karnataka Lingayat Education Society's Parappa Channappa Jabin Science College, Hubli, 580031, Karnataka, India

\* Corresponding author at: Department of Chemistry, Karnatak University, Dharwad 580003, Karnataka, India.

e-mail: [ravichem@kud.ac.in](mailto:ravichem@kud.ac.in) (R.R. Kamble).

## RESEARCH ARTICLE

## ABSTRACT



doi 10.5155/eurjchem.14.1.16-29.2320

Received: 10 August 2022

Received in revised form: 25 November 2022

Accepted: 30 November 2022

Published online: 31 March 2023

Printed: 31 March 2023

## KEYWORDS

Phenothiazine  
 Quantum yield  
 Optical band gap  
 Solvatochromism  
 Cyclic voltammetry  
 Photophysical property

A new class of probes was synthesized using a simple and efficient synthetic protocol. These compounds (PTZ-6(a-e)) have the phenothiazine (PTZ) moiety as the electron donor (D) and substituted aldehydes along with the acrylonitrile group, which acts as the electron acceptor (A), thus making D- $\pi$ -A push-pull system. The structures of the newly synthesized series of small organic target molecules PTZ-6(a-e) were investigated and confirmed by spectroscopic techniques. The optical/solvatochromic properties were studied in detail by UV-vis absorption and fluorescence spectroscopy, because the molecules have shown good solubility in organic solvents. The density functional theory (DFT) model with the CAM-B3LYP function is utilized to study the photophysical properties of the probes, as these probes exhibited orange-to-red emission. Optical band gap values ranged from 2.32 to 2.50 eV, and these probes exhibited good thermal stability with a melting temperature of 136 to 198 °C and a  $T_{5d}$  temperature range from 335 to 354 °C. The cyclic voltammetry study confirms that the  $E_{ox}^{onset}$  values of the target compounds are 0.80 eV. The quantum yields ( $\Phi$ ) of the probes are measured experimentally in ethanol and the Stokes shifts are observed to be in the range of 4846-9430  $\text{cm}^{-1}$ . The results displayed that novel (D-A-D) chromophores could play an important role in organic optoelectronics.

Cite this: *Eur. J. Chem.* 2023, 14(1), 16-29

Journal website: [www.eurjchem.com](http://www.eurjchem.com)

## 1. Introduction

The development of  $\pi$ -conjugated luminescent aromatic and heteroaromatic organic molecules has drawn immense attention of the scientific and industrial communities due to modern applications such as organic light emitting diodes (OLED) [1-3], photovoltaic cells [4,5], lasers [6,7], nonlinear optical (NLO) [8,9], field effect transistors (FET) [10,11], sensors [12], photodetectors [13,14] and bioimaging [15,16]. Organic molecules with donor and acceptor groups in the same molecule that form a push-pull system, among the donor groups, phenothiazine (PTZ) [17,18], carbazole (CZ) [19], triphenylamine (TPA) [20,21], phenoxazine [22] and the acceptor groups, rhodanine [23,24], triazine [25,26], 1,3,4-oxadiazole [27], play the role of forming the push-pull system. During the past two decades  $\pi$ -conjugated amorphous metal-free organic small molecules have been actively used in OLEDs due to their adequate molecular structure, ability to be processed in solution, and vacuum deposition methods along with the use of OLEDs have increased in modern technologies

such as mobile phones, TV, smart watches, laptops, and this is due to properties such as wide viewing angle, low power consumption, better contrast, higher brightness, a wider color range, much faster refresh rates, simpler design that enables ultrathin, flexible, foldable, and transparent displays [1,28-30].

Currently, push-pull systems with the D-A, D- $\pi$ -A, D-A- $\pi$ -A-D strategy increase conjugation in small organic molecules, leading to enhanced absorption and emission properties which are caused by the strong intramolecular charge transfer (ICT) character due to the movement of electrons and holes from the donor to the acceptor groups [31-34]. When a comparison was made between organic photovoltaics (OPV) and inorganic photovoltaics (IPV), inorganic photovoltaics have shown good efficiency, but the cost of OPV is less than that of IPV and is environmentally friendly [35]. The mechanofluorochromic (MFC) properties were also shown by organic molecules with D-A, D- $\pi$ -A, D-A- $\pi$ -A-D strategies that involve PTZ and TPA as core moieties. Mechanofluorochromic (MFC) materials are those that show a change in emission when applying mechanical strength such as grinding, crushing, or rubbing on

organic molecules [36,37]. The mechanofluorochromic property of the molecule depends on the electron accepting capacity of the acceptor, the intermolecular  $\pi$ - $\pi$  interactions, and the steric size of the substituted groups. Strong MFC has been observed by probes that have shorter alkyl chains rather than longer ones [38].

Recently, phenothiazine has received fascinating attention in research fields due to its electron-donating nature, which is due to the presence of electron-rich nitrogen and sulfur [39]. Today, most novel molecules with phenothiazine as a backbone/building blocks show 'aggregation-induced emission' (AIE) along with 'delayed fluorescence' (DF), which plays an important role in optoelectronics, especially in OLEDs [40]. For AIE-DF materials, the twisted structure of PTZ plays an essential role in the separation of the highest occupied molecular orbital (HOMO) and the lowest unoccupied molecular orbital (LUMO), which resulted in a small singlet-triplet (S-T) energy gap [41]. The majority of AIE compounds are blue or green emitters; only a few are red emitters. However, red-emitting AIE probes are important in the fields of OLEDs and bioimaging. These red emissive AIE can be achieved by expanding the  $\pi$ -conjugation length, which can raise the HOMO energy level, and decreasing the LUMO energy level, thus significantly reducing  $E_g$  with higher molecular weights [42].

Based on the ideas mentioned above, we have designed, synthesized, and characterized 3-(4-aminophenyl)acrylonitrile substituted phenothiazines, PTZ-6(a-e). Optoelectronic and photophysical properties, including optical band gap, quantum yield, solvatochromism, intramolecular charge transfer (ICT), and thermal properties of the probes, were investigated thoroughly. The PTZ, being the core moiety, acts as a donor, and the substituted aldehydes along with the cyano group of acrylonitrile act as an acceptor unit, which is located at the third position of the PTZ. The phenyl ring of acrylonitrile acts as an acceptor and as well as  $\pi$ -spacer, forming D- $\pi$ -A push-pulls system that resulted in a larger Stokes shift and good thermal properties. The effect of solvent on the PTZ-6(a-e) probes is carried out to understand the strong ICT and optical property that is aroused by solute solvent interactions. Electrochemical properties were studied by performing cyclic voltammetry in DCM using TBAPF6 as a support electrolyte with a scanning rate of 100 mV/s. DFT studies have been carried out to support the structure-property relationship to corroborate the experimental results. The results obtained agree well with each other, so the synthesized probes PTZ-6(a-e) could play a role in optoelectronics and OLEDs for their application.

## 2. Experimental

### 2.1. Instrumentations

By the open capillary method, the melting points were determined and are uncorrected. FT-IR spectra were recorded using KBr pellets in the Nicolet 5700 FT-IR spectrophotometer instrument. Using the JEOL 400-MHz High Resolution Multinuclear FT-NMR Spectrometer,  $^1\text{H}$  and  $^{13}\text{C}$  nuclear magnetic resonance (NMR) data were collected in  $\text{CDCl}_3$  and  $\text{DMSO-}d_6$  using TMS as internal standard. Chemical shifts are written in ppm downfield ( $\delta$ ). The mass spectra were obtained by the GCMS-QP2010S Shimadzu instrument. Ultraviolet-visible (UV) absorption spectroscopy was recorded using a PerkinElmer Lambda 465 spectrophotometer. Using a JY Horiba, Floromax-4 spectrofluorometer, photoluminescence spectra were recorded. Using CAM-B3LYP/6-311G+(d,p) level of theory in vacuum, DFT calculations were carried out. Differential scanning calorimetry (DSC) and thermogravimetric analysis (TGA) measurements were recorded using a TA Instruments DSC Q20 V24.10 Build 122 and TA Instruments SDT Q600 V20.9 Build 20, respectively, at a heating rate of 10  $^\circ\text{C}/\text{min}$  under nitrogen atmosphere.

### 2.2. Materials

All required precursor chemicals are reagent-/analytical grade and used without any further purification. Catalyst and substituted aryl aldehydes were purchased from Sigma-Aldrich. All solvents used for analytical measurements and preparation were freshly distilled over drying reagents prior to use. The required key intermediates 10-propyl-10H-phenothiazine, 10-propyl-10H-phenothiazine-3-carbaldehyde, (Z)-2-(4-nitrophenyl)-3-(10-propyl-10H-phenothiazin-7-yl)-acrylonitrile and the precursor compound PTZ-4 were synthesized according to the literature [34,39-41].

### 2.3. Synthesis

#### 2.3.1. Synthesis of intermediates

##### 2.3.1.1. 10-Propyl-10H-phenothiazine (PTZ-1)

To a cooled solution of phenothiazine (5.0 g, 2.51 mmol) at 0-5  $^\circ\text{C}$  in DMF, NaH (0.60 g, 1.44 mmol) was slowly added, after complete addition of NaH, 1-bromopropane (3.06 g, 2.51 mmol) was added dropwise and stirred at room temperature overnight. The completion of the reaction was monitored by TLC. After completion of the reaction, the reaction mixture was quenched in ice water and extracted twice in hexane and dried over anhydrous magnesium sulphate, the solvent was evaporated under reduced pressure using rotavapor to obtain the intermediate 10-propyl-10H-phenothiazine (PTZ-1) with 95% yield (Scheme 1).

##### 2.3.1.2. 10-Propyl-10H-phenothiazine-3-carbaldehyde (PTZ-2)

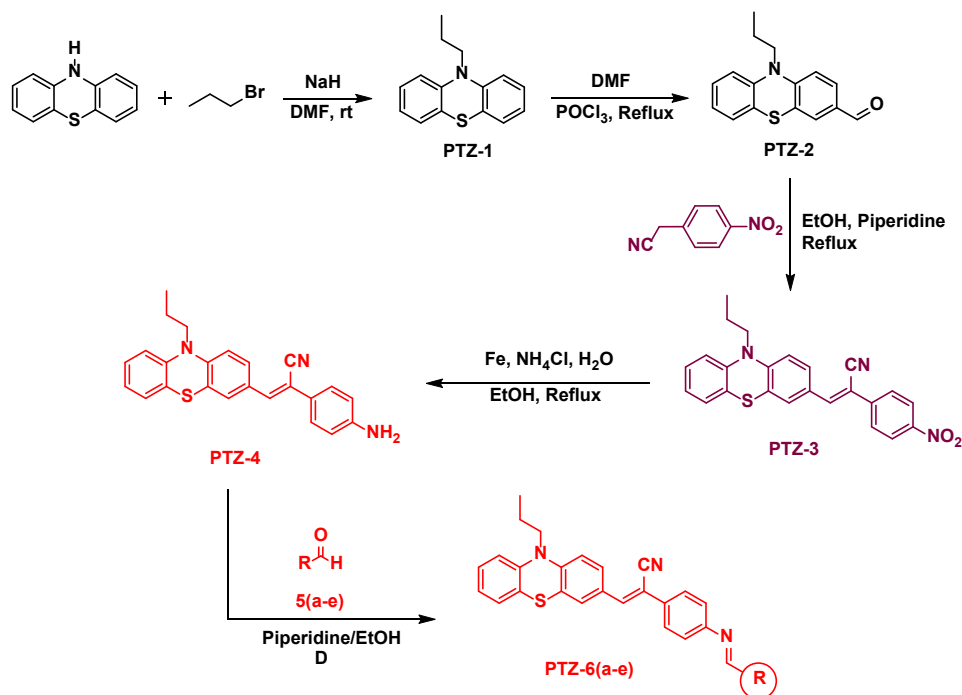
To a solution of DCE and DMF (1.51 g, 2.0 mmol) in an ice bath, phosphoryl chloride (3.18 g, 2.0 mmol) was added drop wise, after complete addition, (PTZ-1) (5.0 g, 2.0 mmol) in DCE was slowly added, then the reaction was heated to reflux and kept overnight and the reaction is confirmed by TLC. The reaction mixture was then added to ice water and extracted with  $\text{CHCl}_3$  ( $3 \times 20$  mL). The organic layer was dried over anhydrous  $\text{MgSO}_4$  and then the solvent was removed in vacuum to obtain 10-propyl-10H-phenothiazine-3-carbaldehyde (PTZ-2) with a 90% yield (Scheme 1).

##### 2.3.1.3. (Z)-2-(4-Nitrophenyl)-3-(10-propyl-10H-phenothiazin-7-yl) acrylonitrile (PTZ-3)

A solution of 10-propyl-10H-phenothiazine-3-carbaldehyde (PTZ-2) (5.0 g, 1.85 mmol) and 2-(4-nitrophenyl)acetonitrile (3.0 g, 1.85 mmol) in ethanol (20.0 mL) was stirred at room temperature. Piperidine (1.57 g, 1.85 mmol) was then added and the mixture was heated to reflux for 4 h. The reaction was confirmed by TLC, and then the reaction mixture was cooled to room temperature and filtered, washed with cold ethanol to obtain intermediate (Z)-2-(4-nitrophenyl)-3-(10-propyl-10H-phenothiazin-7-yl) acrylonitrile (PTZ-3) with 95% yield according to the procedure reported (Scheme 1).

##### 2.3.1.4. (Z)-2-(4-Aminophenyl)-3-(10-propyl-10H-phenothiazin-7-yl)acrylonitrile (PTZ-4)

To a stirred solution of compound PTZ-3 (5 g, 1.21 mmol) in  $\text{EtOH}/\text{H}_2\text{O}$  (20 mL, 4:1) was added iron powder (38 g, 12.1 mmol) and  $\text{NH}_4\text{Cl}$  (6.54 g, 12.1 mmol). The mixture was refluxed at 80  $^\circ\text{C}$  for 2 h. After confirming the reaction by TLC, the reaction mixture was filtered through a pad of celite, washed with  $\text{EtOAc}$  ( $3 \times 50$  mL), and then the solvent layer was passed through  $\text{Na}_2\text{SO}_4$ .



Scheme 1. Synthetic procedure for the compounds PTZ-6(a-e).

The organic layer was concentrated under reduced pressure to obtain the intermediate (*Z*)-2-(4-aminophenyl)-3-(10-propyl-10*H*-phenothiazin-7-yl) acrylonitrile (PTZ-4) with 90% yield according to the procedure reported (Scheme 1).

### 2.3.2. Synthesis of PTZ-6(a-e)

To a mixture of intermediate (*Z*)-2-(4-aminophenyl)-3-(10-propyl-10*H*-phenothiazin-7-yl) acrylonitrile (PTZ-4) (3.0 g, 0.78 mmol) and aryl aldehydes 5a-e (0.95 g, 0.78 mmol) were added in EtOH (20 mL) in the presence of a catalytic amount of acetic acid. The reaction mixture was refluxed for 4 hours at 80 °C. The progress of the reaction was monitored by TLC. After the completion of the reaction, the reaction mixture was filtered, washed with ethanol and dried to obtain the target compounds PTZ-6(a-e) with a yield of 85-90% (Scheme 1).

(*Z*)-2-(4-(((*E*)-2-Hydroxynaphthalen-1-yl) methylene) amino) phenyl)-3-(10-propyl-10*H*-phenothiazin-3-yl)acrylonitrile (PTZ-6a): Color: Orange red. Yield: 89%. M.p.: 188-189 °C. FT-IR (KBr,  $\nu$ ,  $\text{cm}^{-1}$ ): 3449 (OH, naphthaldehyde), 3063 (CH aromatic), 2969, 2927 (CH aliphatic), 2209 (CN aliphatic), 1622, 1595 (C=C and C=N imine), 740 (C-S-C stretching, phenothiazine ring).  $^1\text{H}$  NMR (400 MHz, DMSO- $d_6$ ,  $\delta$ , ppm): 9.62 (s, 1H, -N=CH), 8.45 (d,  $J$  = 8.5 Hz, 1H, Ar-H), 7.90-7.84 (m, 2H, Ar-H), 7.77 (m, 4H, Ar-H, CN-C=C-H, Ph-OH), 7.69 (m, 4H, H-Ar-N=), 7.51 (t,  $J$  = 7.4 Hz, 1H, Ar-H), 7.30 (t,  $J$  = 7.4 Hz, 1H, Ar-H), 7.17 (t,  $J$  = 7.7 Hz, 1H, Ar-H), 7.12 (d,  $J$  = 7.5 Hz, 1H, Ar-H), 7.06 (d,  $J$  = 8.8 Hz, 1H, Ar-H), 6.99 (d,  $J$  = 8.1 Hz, 1H, H-Ar-C-S), 6.93 (t,  $J$  = 7.8 Hz, 2H, H-Ar-N), 3.82 (t,  $J$  = 6.9 Hz, 2H, CH<sub>2</sub>-N), 1.73-1.60 (m, 2H, CH<sub>2</sub>-CH<sub>2</sub>-N), 0.91 (t,  $J$  = 7.3 Hz, 3H, CH<sub>3</sub>-(CH<sub>2</sub>)<sub>2</sub>-N).  $^{13}\text{C}$  NMR (100 MHz, DMSO- $d_6$ ,  $\delta$ , ppm): 171.78, 155.59, 147.09, 144.39, 144.38, 143.87, 141.24, 137.82, 133.66, 132.45, 129.85, 129.58, 128.72, 128.41, 128.09, 127.75, 127.21, 127.14, 124.16, 123.69, 122.84, 122.82, 121.58, 121.57, 120.96, 118.80, 116.69, 116.17, 109.21, 106.86, 48.96, 19.94, 11.45. GC/MS (EI,  $m/z$  (%)) calculated for C<sub>35</sub>H<sub>27</sub>N<sub>3</sub>OS: 537.19; found: 537.68 (M<sup>+</sup>). Anal. calcd. for C<sub>35</sub>H<sub>27</sub>N<sub>3</sub>OS: C, 78.18; H, 5.06; N, 7.82. Found: C, 78.14; H, 5.01; N, 7.80%.

(*Z*)-2-(4-(((*E*)-4-(Diethylamino)-2-hydroxy benzylidene) amino) phenyl)-3-(10-propyl-10*H*-phenothiazin-3-yl) acrylonitrile (PTZ-6b): Color: Brick red. Yield: 85%. M.p.: 164-165 °C. FT-IR (KBr,  $\nu$ ,  $\text{cm}^{-1}$ ): 3444 (OH, aldehyde), 2974 (CH aromatic), 2926, 2852 (CH aliphatic), 2210 (CN aliphatic), 1636, 1559 (C=C and C=N imine), 719 (C-S-C stretching, phenothiazine ring).  $^1\text{H}$  NMR (400 MHz, CDCl<sub>3</sub>,  $\delta$ , ppm): 8.17 (s, 1H, -N=CH), 7.71 (dd,  $J$  = 8.7, 2.3 Hz, 1H, H-Ar-C=C-N), 7.61 (d,  $J$  = 8.8 Hz, 2H, CN-CH<sub>2</sub>-Ar-H), 7.55 (d,  $J$  = 2.3 Hz, 1H, -CH<sub>2</sub>-Ar-H), 7.29 (d,  $J$  = 3.3 Hz, 1H, H-Ar-CH=C-S), 7.27-7.21 (m, 3H, H-Ar-CH=C-N), 7.12 (t,  $J$  = 6.9 Hz, 1H, H-Ar-CH=CH=C-N), 7.06 (d,  $J$  = 7.7 Hz, 1H, H-Ar-C-N), 6.91 (t,  $J$  = 7.5 Hz, 1H, Ar-H), 6.80 (dd,  $J$  = 8.4, 3.3 Hz, 2H, H-Ar-C-S), 6.57 (s, 1H, HO-C-Ar-H), 6.28 (dd,  $J$  = 9.3, 2.4 Hz, 1H, H-Ar-C-N-CH<sub>2</sub>), 4.98 (s, 1H, Ph-OH), 3.77 (t,  $J$  = 7.2 Hz, 2H, CH<sub>2</sub>-N), 3.38 (q,  $J$  = 7.2 Hz, 4H, -(CH<sub>2</sub>)<sub>2</sub>-N), 1.79 (p,  $J$  = 7.3 Hz, 2H, CH<sub>2</sub>-CH<sub>2</sub>-N), 1.19 (t,  $J$  = 7.1 Hz, 6H, (CH<sub>3</sub>)<sub>2</sub>-(CH<sub>2</sub>)<sub>2</sub>-N), 0.99 (t,  $J$  = 7.3 Hz, 3H, CH<sub>3</sub>-(CH<sub>2</sub>)<sub>2</sub>-N).  $^{13}\text{C}$  NMR (100 MHz, CDCl<sub>3</sub>,  $\delta$ , ppm): 166.50, 157.36, 152.02, 147.49, 143.69, 141.14, 138.41, 137.61, 133.51, 129.36, 128.29, 127.56, 127.27, 124.75, 123.52, 123.29, 118.62, 118.21, 115.70, 115.14, 107.92, 106.43, 106.28, 98.07, 49.56, 45.83, 20.04, 12.78, 11.32. GC/MS (EI,  $m/z$  (%)) calculated for C<sub>35</sub>H<sub>34</sub>N<sub>4</sub>OS: 558.25; found: 558.74 (M<sup>+</sup>). Anal. calcd. for C<sub>35</sub>H<sub>34</sub>N<sub>4</sub>OS: C, 75.24; H, 6.13; N, 10.03. Found: C, 75.21; H, 6.10; N, 10.01%.

(*Z*)-2-(4-(((*E*)-2-Hydroxy-5-methoxy benzylidene) amino) phenyl)-3-(10-propyl-10*H*-phenothiazin-3-yl)acrylonitrile (PTZ-6c): Color: Dark yellow. Yield: 85%. M.p.: 129-130 °C. FT-IR (KBr,  $\nu$ ,  $\text{cm}^{-1}$ ): 3445 (OH, aldehyde), 3055 (CH aromatic), 2962, 2930, 2872 (CH aliphatic), 2210 (CN aliphatic), 1621, 1587 (C=C and C=N imine), 745 (C-S-C stretching, phenothiazine ring).  $^1\text{H}$  NMR (400 MHz, CDCl<sub>3</sub>,  $\delta$ , ppm): 12.66 (s, 1H, Ar-OH), 8.60 (s, 1H, -N=CH), 7.79 (dd,  $J$  = 7.9, 1.5 Hz, 1H, H-Ar-C=C-N), 7.67 (d,  $J$  = 8.7 Hz, 2H, H-Ar-CH<sub>2</sub>-CN), 7.55 (s, 1H, H-Ar-CH=CH-S), 7.35 (s, 1H, CH=C-CN), 7.31 (d,  $J$  = 8.7 Hz, 2H, H-Ar-N=), 7.17-7.12 (m, 1H, Ar-H), 7.10 (dd,  $J$  = 7.6, 1.7 Hz, 1H, H-Ar-C=C-O), 7.00 (dd,  $J$  = 9.0, 2.9 Hz, 1H, H-Ar-CH=C-S), 6.97 (s, 1H, H-Ar-C=C-O), 6.94 (dd,  $J$  = 7.5, 1.2 Hz, 1H, H-Ar-C=C-OH), 6.91-6.89 (m, 1H, Ar-H), 6.85 (d,  $J$  = 8.3 Hz, 2H, H-Ar-C=C-N), 3.85-3.80 (m,

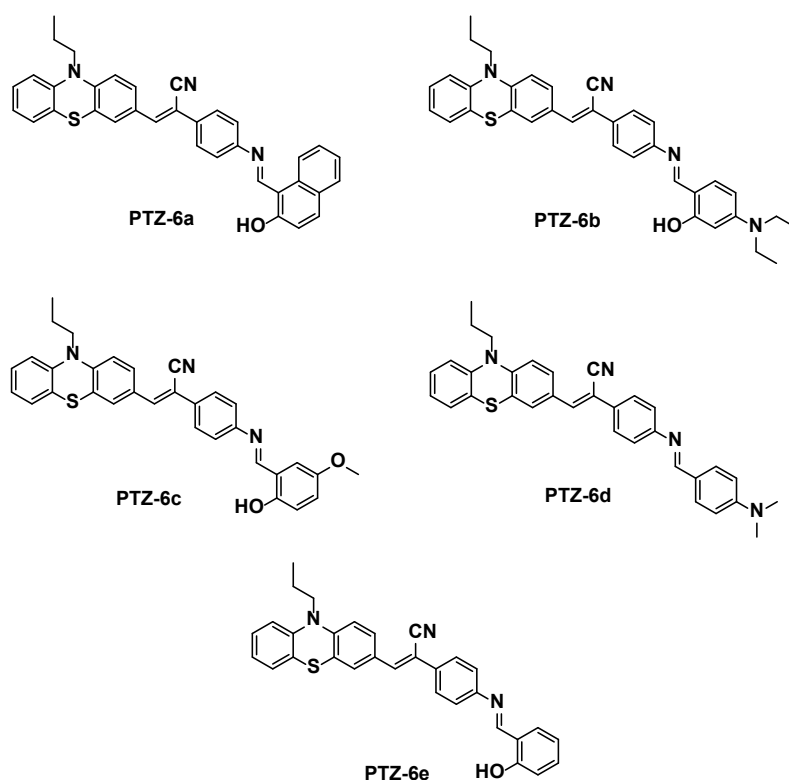


Figure 1. Structure of the final compounds PTZ-6(a-e).

2H, CH<sub>2</sub>-N), 3.80 (s, 3H, O-CH<sub>3</sub>), 1.83 (d, *J* = 7.2 Hz, 2H, CH<sub>2</sub>-CH<sub>2</sub>-N), 1.02 (t, *J* = 7.4 Hz, 3H, CH<sub>3</sub>-(CH<sub>2</sub>)<sub>2</sub>-N). <sup>13</sup>C NMR (100 MHz, CDCl<sub>3</sub>, δ, ppm): 162.74, 155.57, 152.42, 148.74, 147.33, 143.95, 140.64, 133.42, 128.78, 128.57, 127.92, 127.61, 127.58, 126.87, 124.85, 123.75, 123.22, 121.96, 121.05, 118.77, 118.47, 118.27, 115.72, 115.35, 115.24, 107.75, 56.03, 49.53, 20.11, 11.37. GC/MS (EI, *m/z* (%)) calculated for C<sub>32</sub>H<sub>27</sub>N<sub>3</sub>O<sub>2</sub>S: 517.18; found: 517.65 (M<sup>+</sup>). Anal. calcd. for C<sub>32</sub>H<sub>27</sub>N<sub>3</sub>O<sub>2</sub>S: C, 74.25; H, 5.26; N, 8.12. Found: C, 74.21; H, 5.21; N, 8.09%.

(*Z*)-2-(4-(((*E*)-4-(Dimethylamino) benzylidene) amino) phenyl)-3-(10-propyl-10H-phenothiazin-3-yl)acrylonitrile (**PTZ-6d**): Color: Yellow. Yield: 88%. M.p: 128-129 °C. FT-IR (KBr, ν, cm<sup>-1</sup>): 3066 (CH aromatic), 2960, 2925, 2889 (CH aliphatic), 2219 (CN aliphatic), 1606, 1582 (C=C and C=N aromatic), 745 (C-S-C stretching, phenothiazine ring). <sup>1</sup>H NMR (400 MHz, CDCl<sub>3</sub>, δ, ppm): 9.72 (s, 1H, -N=CH), 7.72 (d, *J* = 8.9 Hz, 2H, H-Ar-N=), 7.65 (dd, *J* = 8.7, 2.3 Hz, 1H, H-Ar-C=C-N), 7.54 (d, *J* = 2.1 Hz, 1H, H-Ar-CH=CH-S), 7.48 (d, *J* = 5.3 Hz, 1H, H-Ar-CH<sub>2</sub>-CN), 7.39 (d, *J* = 8.7 Hz, 1H, H-Ar-CH<sub>2</sub>-CN), 7.25 (s, 1H, CH=C-CN), 7.14 (d, *J* = 7.3 Hz, 1H, H-Ar-N=), 7.11 (dd, *J* = 7.6, 1.8 Hz, 1H, Ar-H), 7.06 (d, *J* = 7.5 Hz, 1H, Ar-H), 6.90 (d, *J* = 7.5 Hz, 1H, H-Ar-CH=C-S), 6.83 (d, *J* = 8.9 Hz, 1H, H-Ar-C=C-N), 6.79 (d, *J* = 8.3 Hz, 1H, H-Ar-C=C-N), 6.68 (d, *J* = 9.3 Hz, 2H, H-Ar-N-(CH<sub>3</sub>)<sub>2</sub>), 6.63 (d, *J* = 9.3 Hz, 1H, H-Ar-N=), 3.75 (t, *J* = 7.3 Hz, 2H, CH<sub>2</sub>-N), 3.07 (s, 3H, Ar-N-CH<sub>3</sub>), 3.04 (s, 3H, Ar-N-CH<sub>3</sub>), 1.80 (td, *J* = 14.0, 13.4, 7.3 Hz, 2H, CH<sub>2</sub>-CH<sub>2</sub>-N), 0.98 (t, *J* = 7.3 Hz, 3H, CH<sub>3</sub>-(CH<sub>2</sub>)<sub>2</sub>-N). <sup>13</sup>C NMR (100 MHz, CDCl<sub>3</sub>, δ, ppm): 190.50, 154.43, 138.44, 137.29, 132.12, 129.33, 128.59, 128.16, 127.55, 127.08, 126.85, 126.17, 125.20, 124.79, 124.66, 123.60, 123.21, 123.00, 120.75, 118.71, 115.61, 115.23, 111.08, 49.44, 40.48, 40.21, 20.03, 11.34. GC/MS (EI, *m/z* (%)) calculated for C<sub>33</sub>H<sub>30</sub>N<sub>4</sub>S: 514.22; found: 514.69 (M<sup>+</sup>). Anal. calcd. for C<sub>33</sub>H<sub>30</sub>N<sub>4</sub>S: C, 77.01; H, 5.88; N, 10.89. Found: C, 77.00; H, 5.85; N, 10.86%.

(*Z*)-2-(4-(((*E*)-2-Hydroxybenzylidene)amino)phenyl)-3-(10-propyl-10H-phenothiazin-3-yl)acrylonitrile (**PTZ-6e**): Color:

Orange. Yield: 89%. M.p: 165-166 °C. FT-IR (KBr, ν, cm<sup>-1</sup>): 3442 (OH, aldehyde), 3028 (CH aromatic), 2963, 2925, 2876 (CH aliphatic), 2210 (CN aliphatic), 1617, 1597 (C=C and C=N aromatic), 749 (C-S-C stretching, phenothiazine ring). <sup>1</sup>H NMR (400 MHz, CDCl<sub>3</sub>, δ, ppm): 11.02 (s, 1H, Ar-OH), 8.65 (s, 1H, -N=CH), 7.81 (dd, *J* = 8.7, 2.3 Hz, 1H, H-Ar-C=C-N), 7.68 (d, *J* = 8.7 Hz, 2H, H-Ar-CH<sub>2</sub>-CN), 7.56 (d, *J* = 1.8 Hz, 1H, H-Ar-CH=CH-S), 7.51 (d, *J* = 8.4 Hz, 1H, H-Ar-C-OH), 7.41 (d, *J* = 7.6 Hz, 1H, CH=C=N), 7.35 (d, *J* = 9.0 Hz, 2H, H-Ar-N=), 7.32 (s, 1H, CH=C-CN), 7.15-7.09 (m, 2H, Ar-H), 7.02 (dd, *J* = 7.5, 1.1 Hz, 2H, H-Ar-C=C-N), 6.94 (d, *J* = 7.5 Hz, 1H, H-Ar-CH=C-S), 6.88-6.84 (m, 2H, Ar-H), 3.83 (t, *J* = 7.3 Hz, 2H, CH<sub>2</sub>-N), 1.83 (p, *J* = 7.4 Hz, 2H, CH<sub>2</sub>-CH<sub>2</sub>-N), 1.02 (t, *J* = 7.4 Hz, 3H, CH<sub>3</sub>-(CH<sub>2</sub>)<sub>2</sub>-N). <sup>13</sup>C NMR (100 MHz, CDCl<sub>3</sub>, δ, ppm): 196.75, 163.05, 161.32, 148.66, 147.37, 143.98, 140.68, 137.13, 133.85, 133.70, 132.61, 128.76, 128.59, 127.94, 127.62, 126.91, 124.93, 123.63, 123.23, 121.95, 119.97, 119.36, 118.44, 117.72, 117.44, 115.72, 115.26, 49.54, 20.13, 11.36. GC/MS (EI, *m/z* (%)) calculated for C<sub>31</sub>H<sub>25</sub>N<sub>3</sub>O<sub>2</sub>S: 487.17; found: 487 (M<sup>+</sup>). Anal. calcd. for C<sub>31</sub>H<sub>25</sub>N<sub>3</sub>O<sub>2</sub>S: C, 76.36; H, 5.17; N, 8.62. Found: C, 76.32; H, 5.14; N, 8.60%.

### 3. Results and discussion

#### 3.1. Synthesis and characterization

In the present work, a new class of 4-nitro phenyl acetonitrile containing phenothiazine substituted derivatives was synthesized PTZ-6(a-e) (Figure 1) by adapting a simple and efficient synthetic protocol as shown in Scheme 1. The intermediates required were synthesized according to the literature procedures [38,43-45]. The starting material 10-propyl-10H-phenothiazine (1) was prepared by reacting phenothiazine with 1-bromopropane in the presence of NaH and DMF as solvent. Then 10-propyl-10H-phenothiazine-3-carbaldehyde (2) was synthesized using 10-propyl-10H-phenothiazine, DMF, POCl<sub>3</sub> and DCE, as a solvent using the Vilsmeier-Haack reaction.

**Table 1.** Summary of the optical and thermal properties of  $\pi$ -conjugated molecules PTZ-6(a-e).

| Compounds              | Absorptions<br>$\lambda_{max}^{abs}$ (cm <sup>-1</sup> ) <sup>a</sup> | Emissions<br>$\lambda_{max}^{emi}$ (cm <sup>-1</sup> ) <sup>b</sup> | Stokes<br>shift (cm <sup>-1</sup> ) | $E_g^{opt}$ (eV) <sup>c</sup> | Quantum<br>yield | $T_g/T_m/T_c/T_{5d}$ (°C) <sup>d</sup> |
|------------------------|---|---|-------------------------------------|-------------------------------|------------------|--|
| PTZ-6a                 | 21881   | 17035   | 4846                                | 2.32 (534 nm)                 | 0.040400         | -/198.57/-/335.57                      |
| PTZ-6b                 | 23255   | 17064   | 6191                                | 2.46 (504 nm)                 | 0.001690         | -/171.62/-/290.85                      |
| PTZ-6c                 | 23364   | 16638   | 6726                                | 2.42 (512 nm)                 | 0.000270         | -/136.23/-/350.67                      |
| PTZ-6d                 | 26041   | 16611   | 9430                                | 2.50 (496 nm)                 | 0.001700         | -/136.21/-/353.83                      |
| PTZ-6e                 | 23364   | 16583   | 6781                                | 2.46 (504 nm)                 | 0.000313         | -/172.01/-/346.97                      |
| Reference <sup>e</sup> | 21834   | 17889   | 3945                                | -                             | 0.98             | -                                      |
| Reference <sup>f</sup> | 22675   | 20661   | 2014                                | -                             | 0.80             | -                                      |

<sup>a</sup> The absorption spectra were measured in ethanol at 10  $\mu$ M concentration.

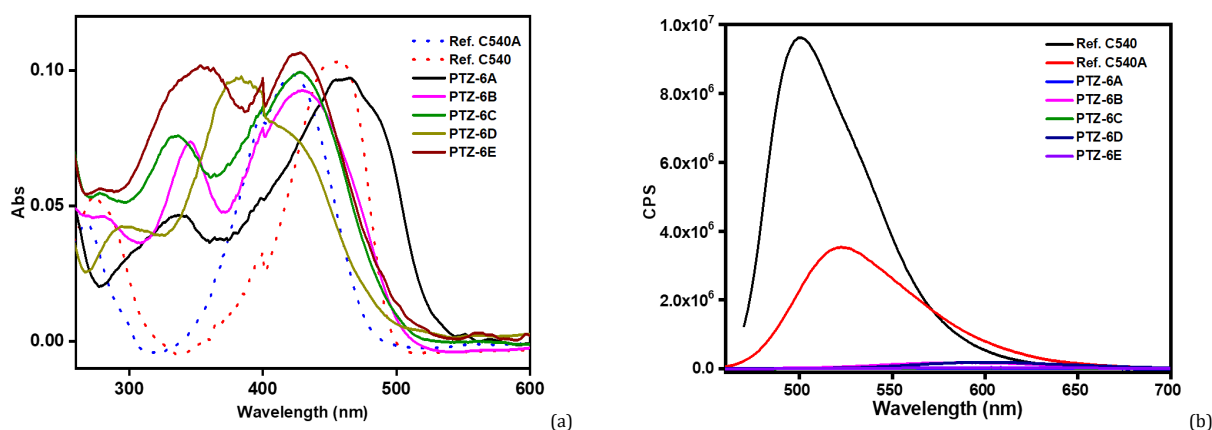
<sup>b</sup> The emission spectra were measured in ethanol at 10  $\mu$ M concentration.

<sup>c</sup> Optical bandgap energies were calculated from  $E_g = hc/\lambda = 1240/\lambda$  (eV).

<sup>d</sup> Obtained from DSC and TGA measurements;  $T_g$ -glass transition temperature,  $T_m$ -melting and  $T_c$ -crystallization temperature, and  $T_{5d}$ -5% weight loss temperature.

<sup>e</sup> Reference, Coumarin 540A [51].

<sup>f</sup> Reference, Coumarin 540 [52].

**Figure 2.** UV-vis absorption (a) and photoluminescence (b) spectra of PTZ-6(a-e) compounds in ethanol at room temperature.

For the compound 2, 4-nitrophenylacetonitrile was condensed in ethanol using piperidine as a base and further followed by reduction using Fe, NH<sub>4</sub>Cl, water, and ethanol according to the literature. In the final step, (Z)-2-(4-amino phenyl)-3-(10-propyl-10H-phenothiazin-7-yl) acrylo nitrile, PTZ-4 reacts with aromatic aldehydes 5a-e to obtain the target compounds PTZ-6(a-e) in the form of Schiff base in the presence of a catalytic amount of acetic acid in ethanol at 80 °C, which is further purified by recrystallization (Yield 85-90%).

The target probes PTZ-6(a-e) are readily soluble in common organic solvents such as chloroform, dichloro-methane, tetrahydrofuran, ethyl acetate and ethanol and can be stored for a longer time without decomposition at ambient temperature. The structures of these novel synthesized small bipolar organic target molecules PTZ-6(a-e) were confirmed by spectroscopic techniques such as <sup>1</sup>H NMR, <sup>13</sup>C NMR, FT-IR, and GC-MS. The results obtained were found to agree well with the proposed structure of the target compounds PTZ-6(a-e).

### 3.2. Photophysical properties

#### 3.2.1. Optical properties

UV-Vis absorption and photoluminescence (PL) spectroscopy techniques were used to investigate the photophysical properties of the designed compounds PTZ-6(a-e) in ethanol at room temperature. All five dyes showed two distinguishable absorption bands, which are shown in Figure 2. The higher energy absorption band appearing within 310-330 nm was attributed to the localized  $\pi$ - $\pi^*$  electronic transitions of phenothiazine and substituted aldehydes, even when no conjugation break was observed. The lower energy absorption band from 384 to 457 nm is assigned to the delocalized  $\pi$ - $\pi^*$  electronic transition which stems from the intramolecular charge transfer of the entire molecular  $\pi$ -system [46]. Among

these probes, PTZ-6a has exhibited the highest  $\lambda_{max}^{abs}$  at 457 nm and PTZ-6d exhibited the lowest  $\lambda_{max}^{abs}$  at 384 nm as displayed in Table 1.

The fluorescence quantum yield and electronic properties of the target compounds PTZ-6(a-e) were well explained and displayed by photoluminescence (PL) spectroscopy. It is noticed from Figure 2 that the emission maxima of the PTZ-6(a-e) probes range from 586-603 nm, from which it is evident that these probes emit red fluorescence, which also shows the bathochromic shift and can be attributed to the stronger electron accepting nature of the cyano vinyl and the substituted aldehyde group, thus lowering the HOMO-LUMO band gap [47]. The Stokes shift value ranges from 3945-9430 cm<sup>-1</sup> and this difference in the Stokes shift is due to the substituted aldehydes and results in the fluorescence quantum yield ranging from 0.0404-0.00027 in ethanol (Table 1). This quantum yield of the molecule was due to the stabilization of the excited state by solvent molecules, and relaxation occurs through the charge transfer state radiatively or nonradiatively [48].

#### 3.2.2. Fluorescence quantum yield

The fluorescence quantum yield ( $\Phi_f$ ) in the fields of molecular chemistry and organic electronics is an important parameter because it helps to analyze the quality and efficiency of the developed/constructed light-emitting organic materials. The fluorescence quantum yield is described as the fraction of the number of quanta absorbed by a molecule that are emitted as fluorescence, or, in other words, it is the ratio of photons absorbed to photons emitted through fluorescence [49]. The quantum yield determination provides information on radiation-less processes, coupling of electronic to vibronic states, and excited electronic states [50].

**Table 2.** Summary of the effect of solvent on the molecules PTZ-6(a-e) \*.

| Solvent    | PTZ-6a         |                | Stokes shift, cm <sup>-1</sup> | PTZ-6b         |                | Stokes shift, cm <sup>-1</sup> | PTZ-6c         |                | Stokes shift, cm <sup>-1</sup> | PTZ-6d         |                | Stokes shift, cm <sup>-1</sup> | PTZ-6e         |                | Stokes shift, cm <sup>-1</sup> |
|------------|----------------|----------------|--------------------------------|----------------|----------------|--------------------------------|----------------|----------------|--------------------------------|----------------|----------------|--------------------------------|----------------|----------------|--------------------------------|
|            | λ <sub>a</sub> | λ <sub>f</sub> |                                | λ <sub>a</sub> | λ <sub>f</sub> |                                | λ <sub>a</sub> | λ <sub>f</sub> |                                | λ <sub>a</sub> | λ <sub>f</sub> |                                | λ <sub>a</sub> | λ <sub>f</sub> |                                |
| Methanol   | 459            | 581            | 4575                           | 441            | 580            | 5435                           | 424            | 581            | 6373                           | 402            | 582            | 7693                           | 422            | 583            | 6544                           |
| Hexanol    | 462            | 595            | 4839                           | 435            | 593            | 6125                           | 430            | 597            | 6505                           | 381            | 590            | 9297                           | 429            | 600            | 6644                           |
| Octanol    | 462            | 565            | 3946                           | 462            | 579            | 4374                           | 431            | 559            | 5312                           | 431            | 576            | 5344                           | 428            | 559            | 5475                           |
| Decanol    | 460            | 563            | 3978                           | 460            | 567            | 4103                           | 432            | 558            | 5227                           | 382            | 580            | 8937                           | 429            | 558            | 5389                           |
| DMSO       | 464            | 577            | 4220                           | 435            | 616            | 6755                           | 435            | 580            | 5747                           | 392            | 615            | 9250                           | 433            | 580            | 5853                           |
| DMF        | 447            | 572            | 4889                           | 429            | 610            | 6917                           | 429            | 573            | 5858                           | 391            | 607            | 9101                           | 427            | 573            | 5967                           |
| Chloroform | 405            | 602            | 8080                           | 431            | 583            | 6049                           | 378            | 593            | 9592                           | 378            | 562            | 8662                           | 423            | 598            | 6918                           |
| Toluene    | 428            | 573            | 5912                           | 413            | 559            | 6324                           | 431            | 572            | 5719                           | 378            | 554            | 8405                           | 421            | 573            | 6300                           |

\* λ<sub>a</sub>: Absorption maxima in nm; λ<sub>f</sub>: Emission maxima in nm.

In comparison with known quantum yield of the standard dyes, Coumarin 540 (3-(2-benzothiazolyl)-7-(diethylamino)-2H-1-benzopyran-2-one) [51] and Coumarin 540A [52] fluorescence quantum yields (Φ) of PTZ-6(a-e) were measured in ethanol according to Equation (1) at room temperature. The probes were excited at 457, 430, 428, 328, and 428 nm, respectively.

$$\Phi = \Phi_R \frac{I_{OD} n^2}{I_R \frac{OD}{OD} \frac{n^2}{n_R^2}} \quad (1)$$

where *I* is the integrated fluorescence intensity, *OD* is the optical density, and *n* is the refractive index, and the subscript *R* refers to the reference fluorophore of known quantum yield. The quantum yields of the PTZ-6(a-e) probes are in the range 0.00027 to 0.0404 which are close to the reported probes [53] and to the standard cyanine dye (0.012) from the literature [54]. These reports encourage the utilization of these novel probes for their application in optoelectronic devices.

### 3.2.3. Optical band gap

In organic molecules, one of the physical properties, *i.e.*, optical band gap, plays a prominent role in the constructing, better understanding, performance, and functioning of electronic devices. The energy levels of the electronic transitions were measured using a UV or visible spectrophotometer. At resonance, molecules will absorb the quantized energy transported by electromagnetic radiation and promote an electron from the HOMO (low energy molecular orbital) to the LUMO (higher energy molecular orbital) [55,56]. The optical band gap ( $E_g^{opt}$ ) corresponds to the energy of the long wavelength edge of the exciton absorption band [57]. On the contrary, the optical band gap values of the PTZ-6(a-e) dyes were approximated from the onset of the low energy side of their absorption spectra (λ<sub>onset</sub>) to the baseline according to Equation (2) [58] and are shown in Table 1.

$$E_g^{opt} = \frac{1240}{\lambda_{onset}} \quad (2)$$

The optical band gap of the probes ranges from 2.32 to 2.50 eV as tabulated (Table 1). For instance, these values are due to the delocalization of electrons from the donor to the acceptor throughout the π-conjugated molecule, thus lowering the band gap. These low optical band gap values of the PTZ-6(a-e) probes ensure the extension of conjugation, hence leading to the increase in efficiency as well as lifetime of the OLED device. Such a type of bandgap chromophores could be useful in the area of photovoltaic/OLEDs applications.

### 3.2.4. Solvatochromism

In fabricating synthesized molecules for optoelectronic devices, the effect of the solvent on the target probes PTZ-6(a-e) plays a very significant role. As the interaction between the solvent and the solute provides information about the change in the position, intensity, and shape of the absorption and emission bands with the change in the polarity of the solvent.

The changes/variation in bands are due to interactions, which may occur via dipole-dipole interaction, hydrogen bond, charge transfer, or dipole moment reorientation of solvents upon excitation of fluorophores [59,60]. The observed variations in the wavelengths of the excitation and emission bands are attributed to the stability of neither the ground (S<sub>0</sub>) nor the excited state (S<sub>1</sub>) by solvent polarity. It also explains the polar character of the synthesized probes in the ground and excited states while they interact with the solvent [61]. In polar/weakly polar protic solvents (Methanol, hexanol, octanol, decanol) and polar aprotic solvents (DMSO, DMF, chloroform, toluene), the solvent affect is studied for the synthesized probes PTZ-6(a-e) at room temperature to recognize the properties of intramolecular charge transfer (ICT). The results are summarized in Table 2 and displayed in Figures 3 and 4. The small change in spectral shifts, both in excitation and emission maxima, is observed in solvents from methanol to toluene for the probes PTZ-6(a-e) which is caused by the change in the polarity of the solvents along with the specific solvent-solute interaction between -OH of substituted aldehydes and imine of Schiff base with solvents [62,63]. The synthesized molecules PTZ-6(a-e) have shown both bathochromic shifts in polar/weakly polar protic solvents, which implies that the probes are stabilized by solvents in the ground state (S<sub>0</sub>), and hypsochromic shifts in polar aprotic solvents, which confirm that the dye is stabilized in the S<sub>0</sub> or S<sub>1</sub> state depending on the solvent interacted with the solute molecules [64]. In addition, due to the change in solvent polarity, the spectral shifts about 40-50 and 20-30 nm correspond to the absorption and emission bands of the molecules PTZ-6(a-e) [65].

The solvent-solute interaction of PTZ-6(a-e) probes in the excited state resulted in a change in the spectral position and shape in the emission bands. The bathochromic and hypsochromic shifts observed for the probes in the solvent with varying polarity result from differences in the charge distributions of the ground and excited states. Considerably, this is due to the presence of the intramolecular charge transfer between the donor (D) phenothiazine and the acceptor (A) acrylonitrile group along with substituted aldehydes. Interestingly, dual fluorescence is observed for PTZ-6c only in chloroform due to the presence of the hydroxyl group along with the methoxy group, which is incorporated in the aromatic derivative which acquires dissimilar dissociation constants in the ground and excited states [66,67]. These emission bands observed for probe PTZ-6c in chloroform are due to ICT of the electron donor to the electron acceptor and twisted intramolecular charge transfer (TICT); the switched TICT state can be used in sensing [68,69]. Regardless of the probe concentration, the shift of the whole fluorescence band increases the intensity at one of its wings and decreases at the other [70]. Other molecules in the literature also showed dual fluorescence, which are Exalite 404 (E404), Exalite 417 (E417), Exalite 428 (E428), Fluorescein-Na, and Eosine-B [71,72]. The PTZ-6(a-e) probes have shown larger Stokes-shift values ranging from 3946 to 9592 cm<sup>-1</sup> (Table 2), which implies considerably reduced self-absorption and improved fluorescence efficiency.

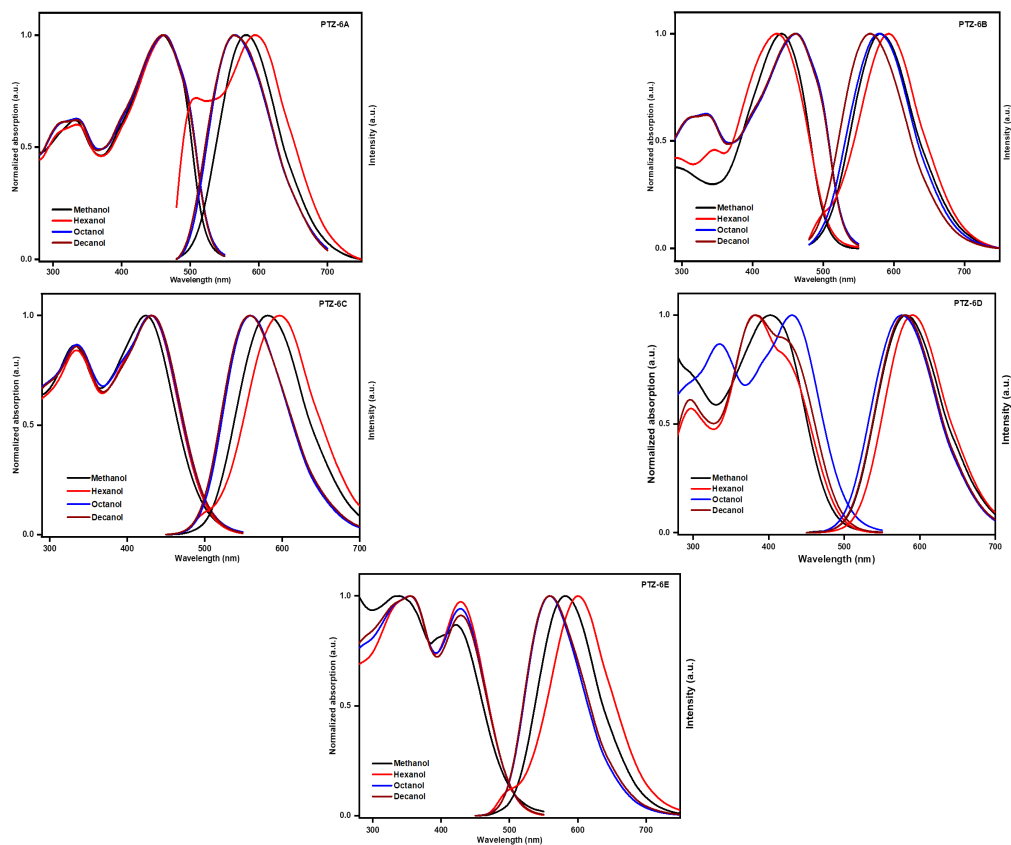


**Figure 3.** Normalized absorption and emission spectra of PTZ-6(a-e) compounds in polar/weakly polar protic solvents such as alcohols.

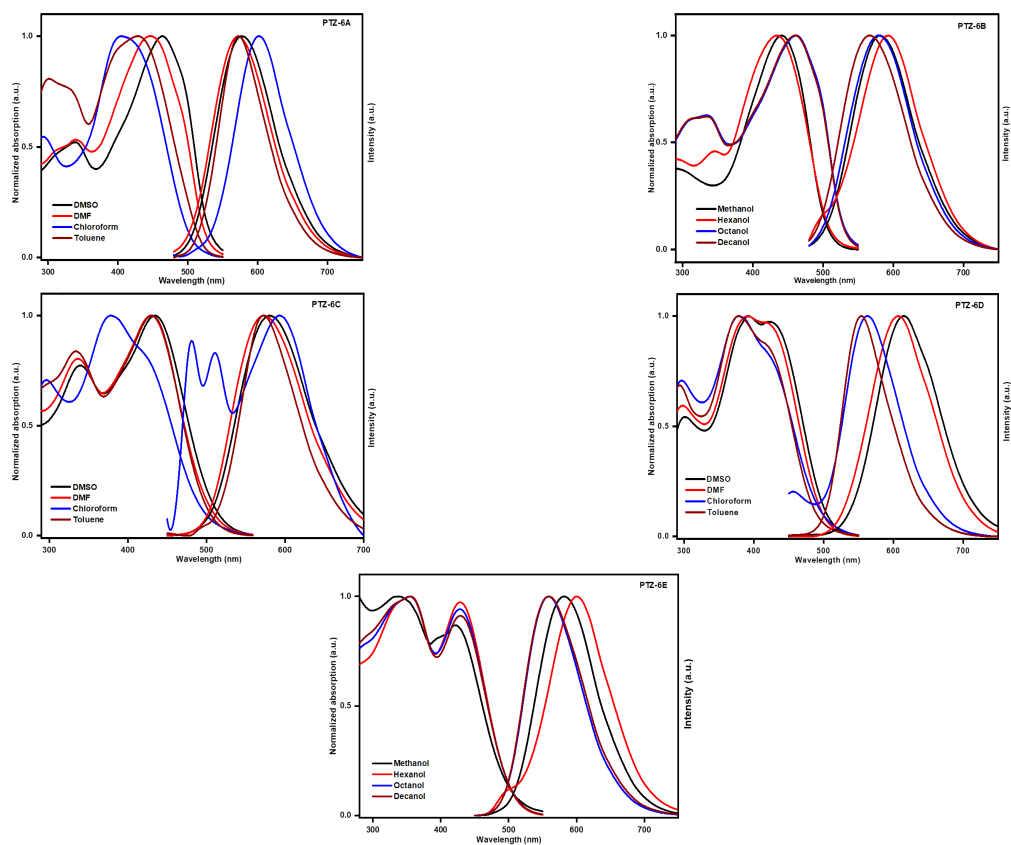


**Figure 4.** Normalized absorption and emission spectra of compounds PTZ-6(a-e) in polar aprotic/nonpolar solvents such as DMSO, DMF, chloroform, and toluene.

**Table 3.** Electrochemical data of the compound PTZ-6(a-e).

| Compound | $E_{ox}^{onset}$ (eV) <sup>a</sup> | $E_{red}^{onset}$ (eV) <sup>a</sup> | HOMO (eV) <sup>b</sup> | LUMO (eV) <sup>c</sup> | $\Delta E$ (eV) <sup>d</sup> | $E_g^{opt}$ (eV) |
|----------|------------------------------------|-------------------------------------|------------------------|------------------------|------------------------------|------------------|
| PTZ-6a   | 0.80                               | 1.00                                | -5.24                  | -3.44                  | 1.80                         | 2.32 (534 nm)    |
| PTZ-6b   | 0.80                               | 1.00                                | -5.24                  | -3.44                  | 1.80                         | 2.46 (504 nm)    |
| PTZ-6c   | 0.80                               | 1.00                                | -5.24                  | -3.44                  | 1.80                         | 2.42 (512 nm)    |
| PTZ-6d   | 0.80                               | 1.00                                | -5.24                  | -3.44                  | 1.80                         | 2.50 (496 nm)    |
| PTZ-6e   | 0.80                               | 1.00                                | -5.24                  | -3.44                  | 1.80                         | 2.46 (504 nm)    |

<sup>a</sup> Onset potential relative to the Ag/AgCl electrode.

<sup>b</sup> Calculated HOMO from the onset oxidation potentials  $HOMO = - [E_{ox}^{onset} + 4.44]$  (eV).

<sup>c</sup> Calculated LUMO using onset reduction potentials  $LUMO = - [E_{red}^{onset} + 4.44]$  (eV).

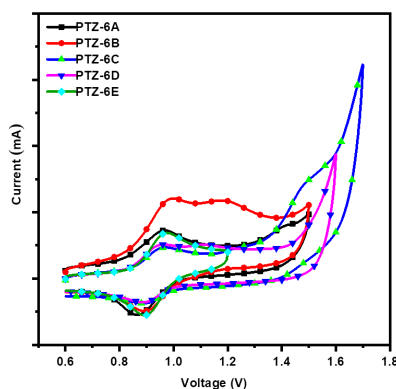
<sup>d</sup> Energy band gap calculated from CV.

**Table 4.** HOMOs, LUMOs, and energy gap calculated from DFT model.

| Compounds | HOMO   | LUMO   | $\Delta E$ (eV) <sup>a</sup> | $E_g^{opt}$ (eV) <sup>b</sup> |
|-----------|--------|--------|------------------------------|-------------------------------|
| PTZ-6a    | -5.408 | -2.425 | 2.983                        | 2.32 (534 nm)                 |
| PTZ-6b    | -5.221 | -2.131 | 3.090                        | 2.46 (504 nm)                 |
| PTZ-6c    | -5.827 | -2.343 | 3.484                        | 2.42 (512 nm)                 |
| PTZ-6d    | -5.210 | -2.085 | 3.125                        | 2.50 (496 nm)                 |
| PTZ-6e    | -2.280 | -2.346 | 2.934                        | 2.46 (504 nm)                 |

<sup>a</sup> Band gap obtained using CAM-B3LYP/6-311G (d,p)  $\Delta E = HOMO - LUMO$  (eV).

<sup>b</sup> The optical band gap energies were calculated from the equation  $E_{opt} = hc/\lambda = 1240/\lambda$  (eV), where  $\lambda$  is the edge wavelength (in nm) of the UV-vis absorption spectrum.

**Figure 5.** CV curves of the compounds PTZ-6(a-e) were measured in  $CH_2Cl_2$  in the presence of  $nBu_4NPF_6$  at a scan rate of 100 mV/s.

### 3.3. Electrochemical properties

The electrochemical properties of the synthesized probes PTZ-6(a-e) were investigated by cyclic voltammetry using  $nBu_4NPF_6$  (0.10 M) as a supporting electrolyte with a scanning rate of 100 mV/s in anhydrous DCM solution using the Ag/AgCl electrode as a reference [73]. The onset oxidation potential and the onset reduction potential of PTZ-6(a-e) were estimated to be 0.80 and 1.0 eV (versus Ag/Ag<sup>+</sup>), respectively [74]. Related electrochemical data are tabulated in Table 3 and the voltammograms are shown in Figure 5. The different oxidation and reduction behavior/character have been observed in Figure 5 and it is clear that the molecules show their potential bipolar carrier charge transporting property along with HOMO and LUMO energy levels using the Equations (3) and (4) [75,76].

$$E_{HOMO} = -(E_{ox}^{onset} + 4.44) \text{ eV} \quad (3)$$

$$E_{LUMO} = -(E_{red}^{onset} + 4.44) \text{ eV} \quad (4)$$

The energy band gap values of all probes PTZ-6(a-e) are 1.80 eV, as the HOMO energy level values of all probes are -5.24 eV and the LUMO energy level values are -3.44 eV. The obtained energy band gap results from cyclic voltammetry and absorption are in good agreement.

### 3.4. Computational studies

Density functional theory (DFT) calculations were performed in the gas phase to obtain information on the electronic and geometric structural properties of the target probes PTZ-

6(a-e) by employing at the CAM-B3LYP/6-311G+(d,p) level with Gaussian 16 software [77]. Additionally, the highest occupied molecular orbitals (HOMO), the lowest unoccupied molecular orbitals (LUMO), the molecular electrostatic potential energy surfaces (MEP), and the dihedral angles (DA) of the target molecules PTZ-6(a-e) are investigated by DFT calculations as shown in Figure 6.

From the DFT calculations, the intramolecular charge transfer character, photophysical properties, and distribution of electrons in HOMO and LUMO depict the strength of donor and accepting/anchoring groups in the target molecules PTZ-6(a-e) (Table 4). The HOMOs of these compounds reveal distributions of dispersed electron clouds located at the phenothiazinyl phenyl-acrylonitrile, along with some part over substituted aldehydes in PTZ-6b, and PTZ-6d of the molecules, while the electron clouds of the LUMOs showed the migration of electron clouds over cyano group along with substituted aldehydes in PTZ-6a, PTZ-6c, and PTZ-6d forming D-A-D type system, hence results in increased intramolecular charge transfer character which implicit the electron donating nature of PTZ and accepting nature of cyano and substituted aromatic aldehydes.

The dihedral angle (DA) plays a prime role in deliberating the delocalisation of electrons and structure of the probes; hence it is one key aspect and plays a crucial role in optoelectronics. As Figure 6 shows, the optimized ground-state geometry of the PTZ-6(a-e) molecules and the dihedral angles of the probes around the phenothiazine range from 0.99-38.85° which are tabulated in Table 5.

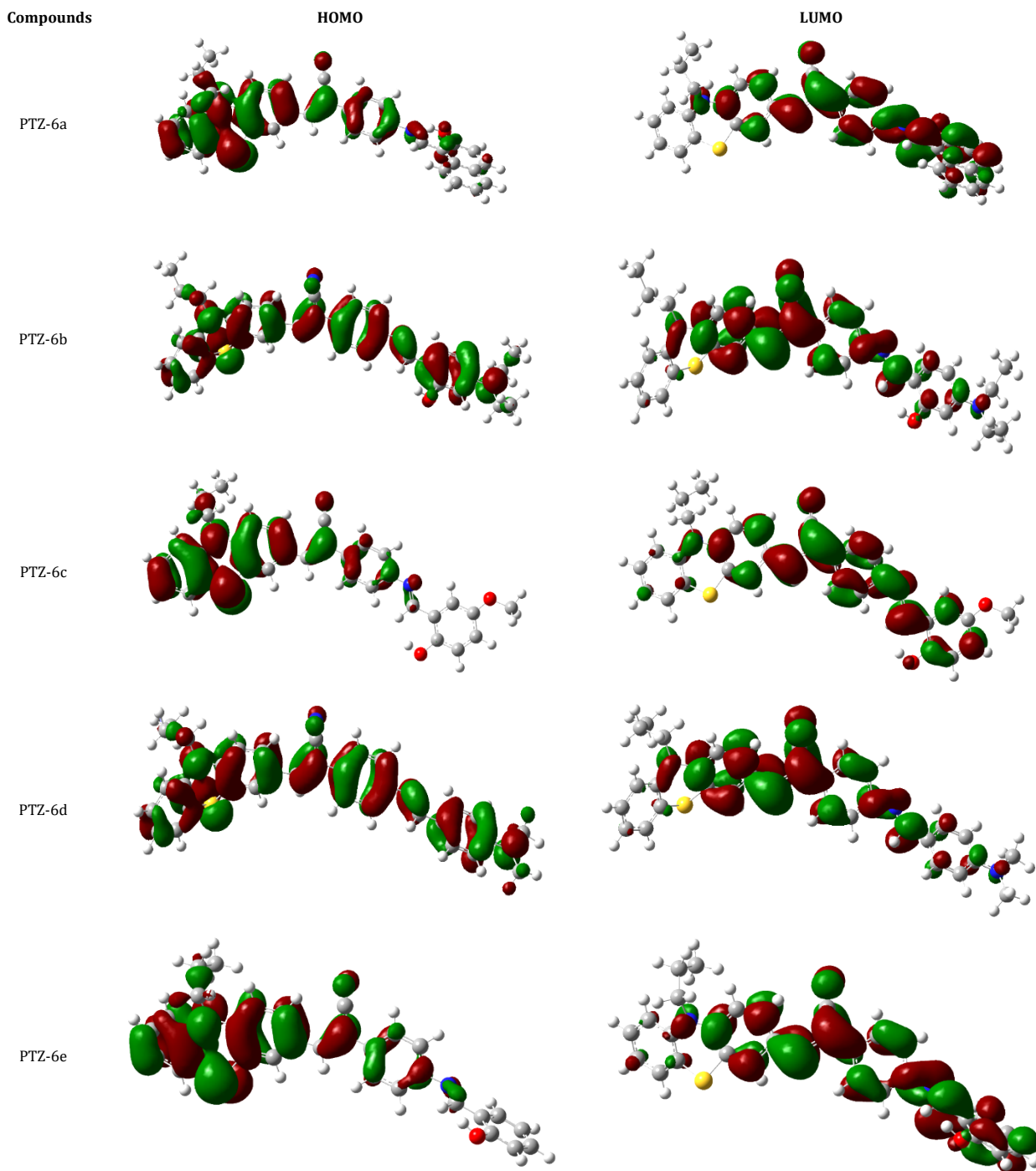


**Figure 6.** Calculated molecular orbital amplitude plots of HOMO and LUMO levels of the compounds PTZ-6(a-e).

The phenothiazine ring exists in a typically 'butterfly-like' confirmation, the conjugation is extended by substituting/linking the acrylonitrile group to phenothiazine, which shows DA of 3.05-7.82° and is almost planar in nature. PTZ-6a exhibited the highest red-shifted absorption maxima (457 nm) among the probes, which are attributed to the higher degree of linear conjugation offered by the chromophores, and therefore the electrons can move from the donor unit to the acceptor unit [1]. This type of planarity of the molecular structure and the dihedral angle between the acceptor and phenothiazine moiety is beneficial for minimizing the HOMO and LUMO which suppress nonradiative decay and enhance radiative efficiency

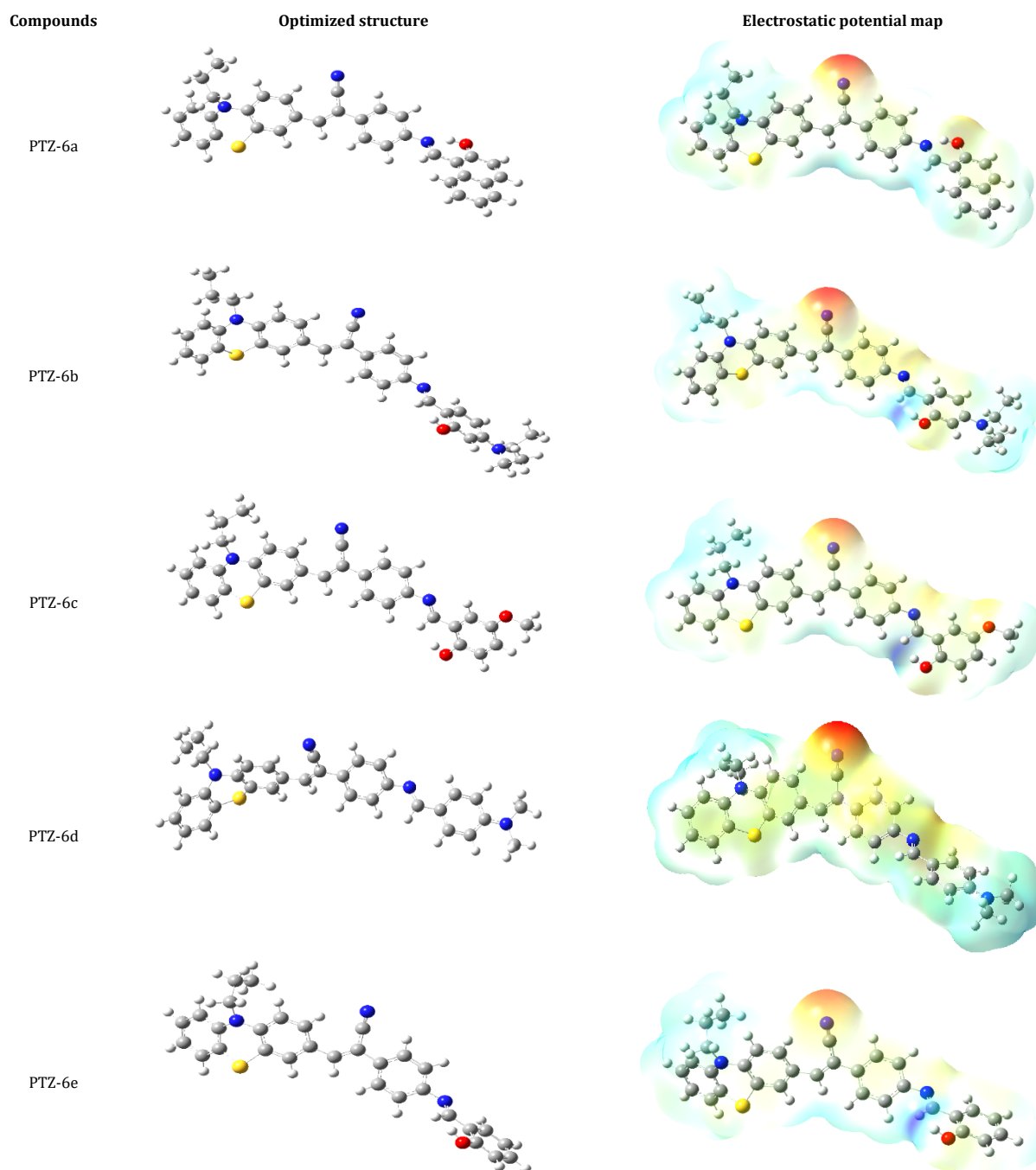
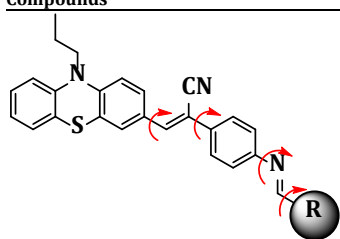
in the solid state, which is beneficial for the fabrication of nondoped OLEDs [78-80].

To better understand the molecular structure, electron transitions, positive, negative, and neutral electrostatic potentials in a better way, molecular electrostatic potential (MEP) plays an important role. The acrylonitrile and salicylaldehydes substituted phenothiazine-based donor- $\pi$ -acceptor PTZ-6(a-e) probes are shown in Figure 7.

The red and blue regions are observed in MEP, which indicates the electron-rich and deficient regions. The red-colored regions on the nitrile group and oxygen in all probes are observed, which indicates the electron-deficient region, and the blue region on the phenothiazine and imine group of Schiff base

**Table 5.** DA: Dihedral angles (°) for PTZ-6(a-e) compounds from ground state (GS) optimized molecular structures.

| Compounds | DA-1 | DA-2  | DA-3  | DA-4 |
|-----------|------|-------|-------|------|
|           | GS   | GS    | GS    | GS   |
| PTZ-6a    | 3.05 | 27.72 | 37.14 | 0.99 |
| PTZ-6b    | 3.15 | 27.23 | 36.81 | 4.97 |
| PTZ-6c    | 6.04 | 27.07 | 35.44 | 8.08 |
| PTZ-6d    | 3.92 | 26.20 | 36.91 | 5.30 |
| PTZ-6e    | 7.82 | 28.02 | 38.85 | 8.38 |

**Figure 7.** Optimized ground state structure and molecular electrostatic potential surfaces of compounds PTZ-6(a-e).

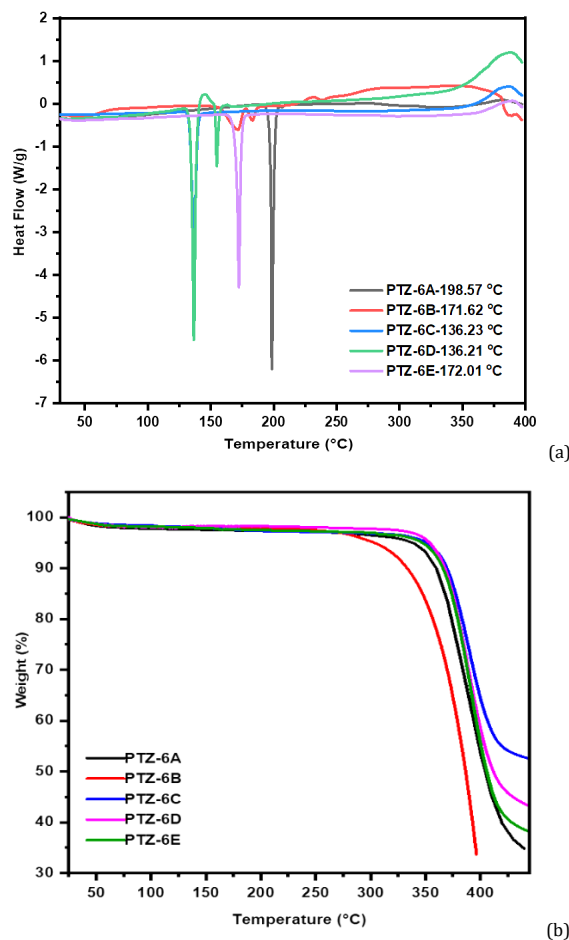


**Figure 8.** (a) DSC and (a) TGA thermograms of the compounds PTZ-6(a-e) at heating rates of 10 °C/min under nitrogen atmosphere.

indicates the electron-rich region. This confirms the presence of the donor- $\pi$ -acceptor strategy in the synthesized probes PTZ-6(a-e) derivatives.

### 3.5. Thermal properties

The morphologically stable thin-film-forming ability of the materials is a crucial need for the successful operation of optoelectronic devices such as OLEDs. From this point of view, the synthesizing materials with a higher glass transition temperature ( $T_g$ ) which helps in generating stable organic devices that ensure no phase transition upon operation. There is a relation between molecular weight and size with the thermal and morphological stability, hence, increasing molecular weight and size by altering different substituents to the host, which could overcome the instability of the probes. The probes PTZ-6(a-e) were investigated by thermal gravimetric analysis (TGA) and differential scanning calorimetry (DSC). Data are tabulated in Table 1 and the results are shown in Figure 8. The DSC was carried out under  $N_2$  from 25-450 °C with a heating rate of 10 °C/min. From the DSC thermogram and phase-transition properties, it is revealed that the compounds are semicrystalline, which shows an endothermic baseline. There is no peak for glass transition temperatures for the probes were observed and the melting temperatures for the probes are ranging from 136.21 to 198.57 °C, among all, PTZ-6a has shown the highest and PTZ-6d has shown the lowest melting temperature. The TGA results recommended that all probes are thermally stable with 5% weight loss temperature

( $T_{5d}$ ) under  $N_2$ , which ranged from 335.57 to 353.83 °C, demonstrating good thermal stability.

### 4. Conclusions

To summarize, we have designed and synthesized phenothiazine-based push-pull chromophores from phenothiazine, 4-nitrophenyl acrylonitrile and aromatic aldehydes by Knoevenagel condensation followed by Schiff base reaction with a simple and efficient protocol in good yield. Photoluminescence spectra and quantum yield (optoelectronic properties) were investigated and found to emit orange to red fluorescence with good quantum yield ( $\phi$ ) and large Stokes shift values. The optical band gap values of these molecules PTZ-6(a-e) were determined from the absorption thresholds and found to be 2.35-2.50 eV. Solvatochromic and DFT studies clearly validate the presence of a strong ICT property, which provides structure-property relationship in a better way. The thermal stability of the chromophores was confirmed by DSC and TGA analysis, and these probes PTZ-6(a-e) exhibited a good  $T_{5d}$  temperature in the range 335.57-353.83 °C. In summary, the results of the compounds studied suggest that the derivatives are potential candidates for applications in the field of organic optoelectronics.

### Acknowledgements

We are thankful to the University Scientific Instrument Centre (USIC) and DST-SAIF, Karnatak University, Dharwad, for providing the spectral data and to the DST-Purse Phase-II program for providing financial support. The authors Mahesh Sadashivappa Najare and Afra-Quasar Nadaf, are thankful to

the University Grants Commission (UGC), New Delhi, India, for providing necessary facilities under UGC-SRF (Sr. No.2121510180 Ref. No. December 20, 2015) and Department of Science and Technology for providing the Inspire Fellowship, respectively.

### Disclosure statement

Conflict of interest: The authors declare that they have no conflict of interest. Ethical approval: All ethical guidelines have been adhered.

Sample availability: Samples of the compounds are available from the author.

### CRedit authorship contribution statement

Conceptualization: Imthiyaz Ahmed Khazi, Ravindra Ramappa Kamble; Methodology: Shivaraj Mantur; Software: Mallikarjun Kalagouda Patil, Shivaraj Mantur; Validation: Mahesh Sadashivappa Najare; Investigation: Shivaraj Mantur; Resources: Mallikarjun Kalagouda Patil; Data Curation: Ravindra Ramappa Kamble; Writing: Shivaraj Mantur; Writing - Review and Editing: Ravindra Ramappa Kamble, Sanjeev Ramchandra Inamdar; Visualization: Mallikarjun Kalagouda Patil, Afra Quasar Nadaf, Mohammed Yaseen, Aravind Raviraj Nesaragi; Funding acquisition: Imthiyaz Ahmed Khazi; Supervision: Ravindra Ramappa Kamble; Project Administration: Imthiyaz Ahmed Khazi.

### ORCID and Email

Shivaraj Mantur

 [shivarajmnr56@gmail.com](mailto:shivarajmnr56@gmail.com)

 <https://orcid.org/0000-0003-4066-0663>

Mallikarjun Kalagouda Patil

 [mkpatilphy@gmail.com](mailto:mkpatilphy@gmail.com)

 <https://orcid.org/0000-0001-7126-9486>

Afra Quasar Abdul Rasheed Nadaf

 [afraqasar@gmail.com](mailto:afraqasar@gmail.com)

 <https://orcid.org/0000-0002-0962-5547>

Mahesh Sadashivappa Najare

 [mahesh.s.najare@gmail.com](mailto:mahesh.s.najare@gmail.com)

 <https://orcid.org/0000-0002-4649-9439>

Mohammed Yaseen

 [yaseen819@gmail.com](mailto:yaseen819@gmail.com)

 <https://orcid.org/0000-0003-1148-4090>

Aravind Raviraj Nesaragi

 [nesaragiaravind@gmail.com](mailto:nesaragiaravind@gmail.com)

 <https://orcid.org/0000-0002-0384-655X>

Sanjeev Ramchandra Inamdar

 [him\\_lax3@yahoo.com](mailto:him_lax3@yahoo.com)

 <https://orcid.org/0000-0003-3398-4897>

Imthiyaz Ahmed Khazi

 [drimkorgchem@gmail.com](mailto:drimkorgchem@gmail.com)

 <https://orcid.org/0000-0001-8216-1913>

Ravindra Ramappa Kamble

 [ravichem@kud.ac.in](mailto:ravichem@kud.ac.in)

 <https://orcid.org/0000-0002-0384-655X>

### References

- [1] Konidena, R. K.; Thomas, K. R. J.; Kumar, S.; Wang, Y.-C.; Li, C.-J.; Jou, J.-H. Phenothiazine decorated carbazoles: effect of substitution pattern on the optical and electroluminescent characteristics. *J. Org. Chem.* **2015**, *80*, 5812–5823.
- [2] Liu, Y.; Li, C.; Ren, Z.; Yan, S.; Bryce, M. R. All-organic thermally activated delayed fluorescence materials for organic light-emitting diodes. *Nat. Rev. Mater.* **2018**, *3*, 18020.
- [3] Zhang, Z.; Zhang, Z.; Chen, R.; Jia, J.; Han, C.; Zheng, C.; Xu, H.; Yu, D.; Zhao, Y.; Yan, P.; Liu, S.; Huang, W. Modulating the optoelectronic properties of large, conjugated, high-energy gap, quaternary phosphine oxide hosts: impact of the triplet-excited-state location. *Chemistry* **2013**, *19*, 9549–9561.
- [4] Sun, X.; Liu, Y.; Xu, X.; Yang, C.; Yu, G.; Chen, S.; Zhao, Z.; Qiu, W.; Li, Y.; Zhu, D. Novel electroactive and photoactive molecular materials based on conjugated donor-acceptor structures for optoelectronic device applications. *J. Phys. Chem. B* **2005**, *109*, 10786–10792.
- [5] Wu, T.-Y.; Tsao, M.-H.; Chen, F.-L.; Su, S.-G.; Chang, C.-W.; Wang, H.-P.; Lin, Y.-C.; Ou-Yang, W.-C.; Sun, I.-W. Synthesis and characterization of organic dyes containing various donors and acceptors. *Int. J. Mol. Sci.* **2010**, *11*, 329–353.
- [6] Jenekhe, S. A.; Lu, L.; Alam, M. M. New conjugated polymers with Donor-Acceptor architectures: Synthesis and photophysics of Carbazole-Quinoline and Phenothiazine-Quinoline copolymers and oligomers exhibiting large intramolecular charge transfer. *Macromolecules* **2001**, *34*, 7315–7324.
- [7] Deshapande, N.; Pujar, G. H.; Sunagar, M. G.; Gaonkar, S.; Belavagi, N. S.; Inamdar, S. R.; Bathula, C.; Khazi, I. A. M. Synthesis and optoelectronic exploration of highly conjugated 1,3,4-oxadiazole containing donor- $\pi$ -acceptor chromophores. *ChemistrySelect* **2017**, *2*, 1793–1801.
- [8] Yoon, K. R.; Ko, S.-O.; Lee, S. M.; Lee, H. Synthesis and characterization of carbazole derived nonlinear optical dyes. *Dyes Pigment* **2007**, *75*, 567–573.
- [9] An, Z.-F.; Chen, R.-F.; Yin, J.; Xie, G.-H.; Shi, H.-F.; Tsuboi, T.; Huang, W. Conjugated asymmetric donor-substituted 1,3,5-triazines: new host materials for blue phosphorescent organic light-emitting diodes. *Chemistry* **2011**, *17*, 10871–10878.
- [10] Beaujuge, P. M.; Fréchet, J. M. J. Molecular design and ordering effects in  $\pi$ -functional materials for transistor and solar cell applications. *J. Am. Chem. Soc.* **2011**, *133*, 20009–20029.
- [11] Yuen, J. D.; Kumar, R.; Zakhidov, D.; Seifert, J.; Lim, B.; Heeger, A. J.; Wudl, F. Ambipolarity in benzobisthiadiazole-based donor-acceptor conjugated polymers. *Adv. Mater.* **2011**, *23*, 3780–3785.
- [12] Belavagi, N. S.; Deshapande, N.; Pujar, G. H.; Wari, M. N.; Inamdar, S. R.; Khazi, I. A. M. Design, synthesis and optoelectronic properties of unsymmetrical oxadiazole based indene substituted derivatives as deep blue fluorescent materials. *J. Fluoresc.* **2015**, *25*, 1323–1330.
- [13] Levell, J. W.; Giardini, M. E.; Samuel, I. D. W. A hybrid organic semiconductor/silicon photodiode for efficient ultraviolet photodetection. *Opt. Express* **2010**, *18*, 3219–3225.
- [14] Stiff-Roberts, A. D.; Lantz, K. R.; Pate, R. Room-temperature, mid-infrared photodetection in colloidal quantum dot/conjugated polymer hybrid nanocomposites: a new approach to quantum dot infrared photodetectors. *J. Phys. D Appl. Phys.* **2009**, *42*, 234004.
- [15] Hettiarachchi, S. U.; Prasai, B.; McCarty, R. L. Detection and cellular imaging of human cancer enzyme using a turn-on, wavelength-shiftable, self-immolative profluorophore. *J. Am. Chem. Soc.* **2014**, *136*, 7575–7578.
- [16] Shinar, J.; Shinar, R. Organic light-emitting devices (OLEDs) and OLED-based chemical and biological sensors: an overview. *J. Phys. D Appl. Phys.* **2008**, *41*, 133001.
- [17] Tanaka, H.; Shizu, K.; Nakanotani, H.; Adachi, C. Dual intramolecular charge-transfer fluorescence derived from a phenothiazine-triphenyl-triazine derivative. *J. Phys. Chem. C Nanomater. Interfaces* **2014**, *118*, 15985–15994.
- [18] Lai, R. Y.; Kong, X.; Jenekhe, S. A.; Bard, A. J. Synthesis, cyclic voltammetric studies, and electrogenerated chemiluminescence of a new phenylquinoline-biphenothiazine donor-acceptor molecule. *J. Am. Chem. Soc.* **2003**, *125*, 12631–12639.
- [19] Sych, G.; Volyniuk, D.; Bezikonny, O.; Lytvyn, R.; Grazulevicius, J. V. Dual interface exciplex emission of quinoline and carbazole derivatives for simplified nondoped white OLEDs. *J. Phys. Chem. C Nanomater. Interfaces* **2019**, *123*, 2386–2397.
- [20] Seok, J. H.; Park, S. H.; El-Khouly, M. E.; Araki, Y.; Ito, O.; Kay, K.-Y. Photoinduced processes of newly synthesized bisferrocene- and bisfullerene-substituted tetrads with a triphenylamine central block. *J. Organomet. Chem.* **2009**, *694*, 1818–1825.
- [21] El-Khouly, M. E.; Kim, J. H.; Kwak, M.; Choi, C. S.; Ito, O.; Kay, K.-Y. Photoinduced charge separation of the covalently linked fullerene-triphenylamine-fullerene triad. Effect of dual fullerenes on lifetimes of charge-separated states. *Bull. Chem. Soc. Jpn.* **2007**, *80*, 2465–2472.
- [22] Qiu, X.; Shi, J.; Xu, X.; Lu, Y.; Sun, Q.; Xue, S.; Yang, W. Tuning the optoelectronic properties of phenothiazine-based D-A-type emitters through changing acceptor pattern. *Dyes Pigment* **2017**, *147*, 6–15.
- [23] Avhad, K. C.; Patil, D. S.; Chitrambalam, S.; Sreenath, M. C.; Joe, I. H.; Sekar, N. Extensive study of rhodanine-arylamine-based chromophores: Consolidated optical, DFT/TD-DFT and non-linear optical properties. *ChemistrySelect* **2019**, *4*, 211–221.
- [24] Madrid-Úsuga, D.; Melo-Luna, C. A.; Insuastry, A.; Ortiz, A.; Reina, J. H. Optical and electronic properties of molecular systems derived from rhodanine. *J. Phys. Chem. A* **2018**, *122*, 8469–8476.
- [25] Lee, Y.; Woo, S.-J.; Kim, J.-J.; Hong, J.-I. Blue thermally activated delayed fluorescence emitter using modulated triazines as electron acceptors. *Dyes Pigment* **2020**, *172*, 107864.
- [26] Youn Lee, S.; Yasuda, T.; Nomura, H.; Adachi, C. High-efficiency organic light-emitting diodes utilizing thermally activated delayed fluorescence from triazine-based donor-acceptor hybrid molecules. *Appl. Phys. Lett.* **2012**, *101*, 093306.
- [27] Cooper, M. W.; Zhang, X.; Zhang, Y.; Jeon, S. O.; Lee, H.; Kim, S.; Fuentes-Hernandez, C.; Barlow, S.; Kippelen, B.; Marder, S. R. Effect of the number and substitution pattern of carbazole donors on the singlet and triplet state energies in a series of carbazole-oxadiazole

- derivatives exhibiting thermally activated delayed fluorescence. *Chem. Mater.* **2018**, *30*, 6389–6399.
- [28]. Huang, Z.-S.; Meier, H.; Cao, D. Phenothiazine-based dyes for efficient dye-sensitized solar cells. *J. Mater. Chem. C Mater. Opt. Electron. Devices* **2016**, *4*, 2404–2426.
- [29]. Huh, J. W.; Kim, Y. M.; Park, Y. W.; Choi, J. H.; Lee, J. W.; Lee, J. W.; Yang, J. W.; Ju, S. H.; Paek, K. K.; Ju, B. K. Characteristics of organic light-emitting diodes with conducting polymer anodes on plastic substrates. *J. Appl. Phys.* **2008**, *103*, 044502.
- [30]. Karzazi, Y. Organic Light Emitting Diodes: Devices and applications. *J. Mater. Environ. Sci.* **2014**, *5*, 1–12.
- [31]. Zhou, J.; He, B.; Xiang, J.; Chen, B.; Lin, G.; Luo, W.; Lou, X.; Chen, S.; Zhao, Z.; Tang, B. Z. Tuning the AIE activities and emission wavelengths of tetraphenylethene-containing luminogens. *ChemistrySelect* **2016**, *1*, 812–818.
- [32]. Bureš, F. Fundamental aspects of property tuning in push–pull molecules. *RSC Adv.* **2014**, *4*, 58826–58851.
- [33]. Ramakrishna, G.; Goodson, T., 3rd Excited-state deactivation of branched two-photon absorbing chromophores: a femtosecond transient absorption investigation. *J. Phys. Chem. A* **2007**, *111*, 993–1000.
- [34]. Carlotti, B.; Benassi, E.; Spalletti, A.; Fortuna, C. G.; Elisei, F.; Barone, V. Photoinduced symmetry-breaking intramolecular charge transfer in a quadrupolar pyridinium derivative. *Phys. Chem. Chem. Phys.* **2014**, *16*, 13984–13994.
- [35]. Zaier, R.; Hajaji, S.; Kozaki, M.; Ayachi, S. DFT and TD-DFT studies on the electronic and optical properties of linear  $\pi$ -conjugated cyclopentadithiophene (CPDT) dimer for efficient blue OLED. *Opt. Mater. (Amst.)* **2019**, *91*, 108–114.
- [36]. *Mechanochromic fluorescent materials: Phenomena, materials and applications*; Xu, J.; Chi, Z., Eds.; Royal Society of Chemistry: Cambridge, England, 2014.
- [37]. Ciardelli, F.; Ruggeri, G.; Pucci, A. Dye-containing polymers: methods for preparation of mechanochromic materials. *Chem. Soc. Rev.* **2013**, *42*, 857–870.
- [38]. Ma, C.; Zhang, X.; Yang, Y.; Ma, Z.; Yang, L.; Wu, Y.; Liu, H.; Jia, X.; Wei, Y. Halogen effect on mechanofluorochromic properties of alkyl phenothiazinyl phenylacrylonitrile derivatives. *Dyes Pigm.* **2016**, *129*, 141–148.
- [39]. Hua, Y.; Chang, S.; Huang, D.; Zhou, X.; Zhu, X.; Zhao, J.; Chen, T.; Wong, W.-Y.; Wong, W.-K. Significant improvement of dye-sensitized solar cell performance using simple phenothiazine-based dyes. *Chem. Mater.* **2013**, *25*, 2146–2153.
- [40]. Data, P.; Takeda, Y. Recent advancements in and the future of organic emitters: TADF- and RTP-active multifunctional organic materials. *Chem. Asian J.* **2019**, *14*, 1613–1636.
- [41]. Huang, L.; Wen, X.; Liu, J.; Chen, M.; Ma, Z.; Jia, X. An AIE molecule featuring changeable triplet emission between phosphorescence and delayed fluorescence by an external force. *Mater. Chem. Front.* **2019**, *3*, 2151–2156.
- [42]. Zhao, Q.; Sun, J. Z. Red and near infrared emission materials with AIE characteristics. *J. Mater. Chem. C Mater. Opt. Electron. Devices* **2016**, *4*, 10588–10609.
- [43]. Mantur, S.; Patil, M. K.; Nadaf, A. A.; Najare, M. S.; Yaseen, M.; Inamdar, S. R.; Khazi, I. A. M. Synthesis, characterization and photophysical properties of  $\pi$ -conjugated novel phenothiazine substituted acrylonitrile D–A derivatives: Orange to red emission. *Chem. Data Coll.* **2020**, *30*, 100543.
- [44]. Park, S. S.; Won, Y. S.; Choi, Y. C.; Kim, J. H. Molecular design of organic dyes with double electron acceptor for dye-sensitized solar cell. *Energy Fuels* **2009**, *23*, 3732–3736.
- [45]. Xu, Y.; Wang, N.-Y.; Song, X.-J.; Lei, Q.; Ye, T.-H.; You, X.-Y.; Zuo, W.-Q.; Xia, Y.; Zhang, L.-D.; Yu, L.-T. Discovery of novel N-(5-(tert-butyl)isoxazol-3-yl)-N'-phenylurea analogs as potent FLT3 inhibitors and evaluation of their activity against acute myeloid leukemia in vitro and in vivo. *Bioorg. Med. Chem.* **2015**, *23*, 4333–4343.
- [46]. Konidena, R. K.; Justin Thomas, K. R.; Singh, M.; Jou, J.-H. Thienylphenothiazine integrated pyrenes: an account on the influence of substitution patterns on their optical and electroluminescence properties. *J. Mater. Chem. C Mater. Opt. Electron. Devices* **2016**, *4*, 4246–4258.
- [47]. Ramachandran, E.; Dhamodharan, R. Rational design of phenothiazine (PTz) and ethylenedioxithiophene (EDOT) based donor-acceptor compounds with a molecular aggregation breaker for solid state emission in red and NIR regions. *J. Mater. Chem. C Mater. Opt. Electron. Devices* **2015**, *3*, 8642–8648.
- [48]. Shanmugasundaram, K.; Subeesh, M. S.; Sunesh, C. D.; Chitumalla, R. K.; Jang, J.; Choe, Y. Green electroluminescence from charged phenothiazine derivative. *J. Phys. Chem. C Nanomater. Interfaces* **2016**, *120*, 20247–20253.
- [49]. Rhys Williams, A. T.; Winfield, S. A.; Miller, J. N. Relative fluorescence quantum yields using a computer-controlled luminescence spectrometer. *Analyst* **1983**, *108*, 1067–1071.
- [50]. Xu, H.; Chen, R.; Sun, Q.; Lai, W.; Su, Q.; Huang, W.; Liu, X. Recent progress in metal-organic complexes for optoelectronic applications. *Chem. Soc. Rev.* **2014**, *43*, 3259–3302.
- [51]. Nedumpara, R. J.; Thomas, K. J.; Jayasree, V. K.; Girijavallabhan, C. P.; Nampoori, V. P. N.; Radhakrishnan, P. Study of solvent effect in laser emission from Coumarin 540 dye solution. *Appl. Opt.* **2007**, *46*, 4786–4792.
- [52]. Drexhage, K. H. Fluorescence efficiency of laser dyes. *J. Res. Natl. Bur. Stand. A Phys. Chem.* **1976**, *80A*, 421.
- [53]. Rodrigues, A. C. B.; Pina, J.; Dong, W.; Forster, M.; Scherf, U.; Seixas de Melo, J. S. Aggregation-induced emission in phenothiazine–TPE and –TPAN polymers. *Macromolecules* **2018**, *51*, 8501–8512.
- [54]. Rurack, K.; Spies, M. Fluorescence quantum yields of a series of red and near-infrared dyes emitting at 600–1000 nm. *Anal. Chem.* **2011**, *83*, 1232–1242.
- [55]. Hu, J.-Y.; Era, M.; Elsegood, M. R. J.; Yamato, T. Synthesis and photophysical properties of pyrene-based light-emitting monomers: Highly pure-blue-fluorescent, cruciform-shaped architectures. *European J. Org. Chem.* **2010**, *2010*, 72–79.
- [56]. Jędrzejewska, B.; Ośmiałowski, B.; Zalesny, R. Application of spectroscopic and theoretical methods in the studies of photoisomerization and photophysical properties of the push-pull styryl-benzimidazole dyes. *Photochem. Photobiol. Sci.* **2016**, *15*, 117–128.
- [57]. Zahn, D. R. T.; Gavrila, G. N.; Gorgoi, M. The transport gap of organic semiconductors studied using the combination of direct and inverse photoemission. *Chem. Phys.* **2006**, *325*, 99–112.
- [58]. Lee, H.; Kim, B.; Kim, S.; Kim, J.; Lee, J.; Shin, H.; Lee, J.-H.; Park, J. Synthesis and electroluminescence properties of highly efficient dual core chromophores with side groups for blue emission. *J. Mater. Chem. C Mater. Opt. Electron. Devices* **2014**, *2*, 4737–4747.
- [59]. Reichardt, C. Solvatochromic dyes as solvent polarity indicators. *Chem. Rev.* **1994**, *94*, 2319–2358.
- [60]. Al-Zahrani, F. A. M. Synthesis, modelling, and solvatochromic properties of a phenothiazine derivative. *Luminescence* **2020**, *35*, 738–747.
- [61]. Gopal, V. R.; Reddy, A. M.; Rao, V. J. Wavelength dependent trans to Cis and quantum chain isomerizations of anthrylethylene derivatives. *J. Org. Chem.* **1995**, *60*, 7966–7973.
- [62]. Slodek, A.; Zych, D.; Maroń, A.; Gawecki, R.; Mrozek-Wilczkiewicz, A.; Malarz, K.; Musioł, R. Phenothiazine derivatives - synthesis, characterization, and theoretical studies with an emphasis on the solvatochromic properties. *J. Mol. Liq.* **2019**, *285*, 515–525.
- [63]. Najare, M. S.; Patil, M. K.; Mantur, S.; Nadaf, A. A.; Inamdar, S. R.; Khazi, I. A. M. Highly conjugated D- $\pi$ -A- $\pi$ -D form of novel benzo[b]thiophene substituted 1,3,4-oxadiazole derivatives; Thermal, optical properties, solvatochromism and DFT studies. *J. Mol. Liq.* **2018**, *272*, 507–519.
- [64]. Rauf, M. A.; Hisaindee, S. Studies on solvatochromic behavior of dyes using spectral techniques. *J. Mol. Struct.* **2013**, *1042*, 45–56.
- [65]. Rout, Y.; Montanari, C.; Pasciucchio, E.; Misra, R.; Carlotti, B. Tuning the fluorescence and the intramolecular charge transfer of phenothiazine dipolar and quadrupolar derivatives by oxygen functionalization. *J. Am. Chem. Soc.* **2021**, *143*, 9933–9943.
- [66]. Laws, W. R.; Brand, L. Analysis of two-state excited-state reactions. The fluorescence decay of 2-naphthol. *J. Phys. Chem.* **1979**, *83*, 795–802.
- [67]. Davenport, L.; Knutson, J. R.; Brand, L. Excited-state proton transfer of equilenin and dihydroequilenin: interaction with bilayer vesicles. *Biochemistry* **1986**, *25*, 1186–1195.
- [68]. El-Kemary, M.; Rettig, W. Multiple emission in coumarins with heterocyclic substituents. *Phys. Chem. Chem. Phys.* **2003**, *5*, 5221–5228.
- [69]. Malval, J. P.; Lapouyade, R.; Léger, J.-M.; Jarry, C. Tripodal ligand incorporating dual fluorescent ionophore: a coordinative control of photoinduced electron transfer. *Photochem. Photobiol. Sci.* **2003**, *2*, 259–266.
- [70]. Demchenko, A. P. The problem of self-calibration of fluorescence signal in microscale sensor systems. *Lab Chip* **2005**, *5*, 1210–1223.
- [71]. Najare, M. S.; Patil, M. K.; Tilakraj, T. S.; Yaseen, M.; Nadaf, A. A.; Mantur, S.; Inamdar, S. R.; Khazi, I. A. M. Photophysical and electrochemical properties of highly  $\pi$ -conjugated bipolar carbazole-1,3,4-oxadiazole-based D- $\pi$ -A type of efficient deep blue fluorescent dye. *J. Fluoresc.* **2021**, *31*, 1645–1664.
- [72]. Huo, H. Asymmetric catalysis with chiral-at-metal complexes: From non-photochemical applications to photoredox catalysis, Presented to the Faculties of Philipps Universität Marburg in Partial Fulfillment: Marburg/Lahn, 2016.
- [73]. Bathula, C.; Badgujar, S.; Belavagi, N. S.; Lee, S. K.; Kang, Y.; Khazi, I. A. M. Synthesis, characterization and optoelectronic properties of benzodithiophene based copolymers for application in solar cells. *J. Fluoresc.* **2016**, *26*, 371–376.
- [74]. Chang, D. W.; Ko, S.-J.; Kim, J. Y.; Dai, L.; Baek, J.-B. Multifunctional quinoxaline containing small molecules with multiple electron-

- donating moieties: Solvatochromic and optoelectronic properties. *Synth. Met.* **2012**, *162*, 1169–1176.
- [75]. Deshapande, N.; Belavagi, N. S.; Sunagar, M. G.; Gaonkar, S.; Pujar, G. H.; Wari, M. N.; Inamdar, S. R.; Khazi, I. A. M. Synthesis, characterization and optoelectronic investigations of bithiophene substituted 1,3,4-oxadiazole derivatives as green fluorescent materials. *RSC Adv.* **2015**, *5*, 86685–86696.
- [76]. Mantur, S.; Patil, M. K.; Najare, M. S.; Nadaf, A. A.; Yaseen, M.; Gaonkar, S.; Inamdar, S. R.; Khazi, I. A. M.; Kamble, R. R. Design and synthesis of D- $\pi$ -A form of p-nitrophenylacrylonitrile substituted triphenylamine chromophores; Photophysical, electrochemical properties, DFT and thermal studies. *ChemistrySelect* **2021**, *6*, 12811–12819.
- [77]. Frisch, M. J.; Trucks, G. W.; Schlegel, H. B.; Scuseria, G. E.; Robb, M. A.; Cheeseman, J. R.; Montgomery, J. A.; Vreven, T.; Kudin, K. N.; Burant, J. C.; Millam, J. M.; Iyengar, S. S.; Tomasi, J.; Barone, V.; Mennucci, B.; Cossi, M.; Scalmani, G.; Rega, N.; Petersson, G. A.; Nakatsuji, H.; Hada, M.; Ehara, M.; Toyota, K.; Fukuda, R.; Hasegawa, J.; Ishida, M.; Nakajima, T.; Honda, Y.; Kitao, O.; Nakai, H.; Klene, M.; Li, X.; Knox, J. E.; Hratchian, H. P.; Cross, J. B.; Adamo, C.; Jaramillo, J.; Gomperts, R.; Stratmann, R. E.; Yazyev, O.; Austin, A. J.; Cammi, R.; Pomelli, C.; Ochterski, J. W.; Ayala, P. Y.; Morokuma, K.; Voth, G. A.; Salvador, P.; Dannenberg, J. J.; Zakrzewski, V. G.; Dapprich, S.; Daniels, A. D.; Strain, M. C.; Farkas, O.; Malick, D. K.; Rabuck, A. D.; Raghavachari, K.; Foresman, J. B.; Ortiz, J. V.; Cui, Q.; Baboul, A. G.; Clifford, S.; Cioslowski, J.; Stefanov, B. B.; Liu, G.; Liashenko, A.; Piskorz, P.; Komaromi, I.; Martin, R. L.; Fox, D. J.; Keith, T.; Al-Laham, M. A.; Peng, C. Y.; Nanayakkara, A.; Challacombe, M.; Gill, P. M. W.; Johnson, B.; Chen, W.; Wong, M. W.; Gonzalez, C.; Pople, J. A. Gaussian, Inc., Wallingford CT, 2004.
- [78]. Li, D.-M.; Zhou, H.-P.; Pu, J.-Q.; Feng, X.-J.; Wu, J.-Y.; Tian, Y.-P.; Yu, X.-Q.; Tao, X.-T.; Jiang, M.-H. Synthesis, luminescence and electrochemical properties of two phenothiazine derivatives. *Chin. J. Chem.* **2005**, *23*, 1483–1489.
- [79]. Jin, R.; Tang, S. Theoretical study on optical and electronic properties of bipolar molecules with 1,8-naphthalimide and triphenylamine moieties as organic light-emitting materials. *J. Mol. Graph. Model.* **2013**, *42*, 120–128.
- [80]. Shen, Y.-F.; Li, M.; Zhao, W.-L.; Wang, Y.-F.; Lu, H.-Y.; Chen, C.-F. Quinoline-based TADF emitters exhibiting aggregation-induced emission for efficient non-doped organic light-emitting diodes. *Mater. Chem. Front.* **2021**, *5*, 834–842.



Copyright © 2023 by Authors. This work is published and licensed by Atlanta Publishing House LLC, Atlanta, GA, USA. The full terms of this license are available at <http://www.eurjchem.com/index.php/eurjchem/pages/view/terms> and incorporate the Creative Commons Attribution-Non Commercial (CC BY NC) (International, v4.0) License (<http://creativecommons.org/licenses/by-nc/4.0>). By accessing the work, you hereby accept the Terms. This is an open access article distributed under the terms and conditions of the CC BY NC License, which permits unrestricted non-commercial use, distribution, and reproduction in any medium, provided the original work is properly cited without any further permission from Atlanta Publishing House LLC (European Journal of Chemistry). No use, distribution, or reproduction is permitted which does not comply with these terms. Permissions for commercial use of this work beyond the scope of the License (<http://www.eurjchem.com/index.php/eurjchem/pages/view/terms>) are administered by Atlanta Publishing House LLC (European Journal of Chemistry).